# Monitoring Bus Passenger Zonal Origin-Destination Matrices: Development, Validation, and Application Using Data from The Ohio State University Campus Area Bus System

Thesis

Presented in Partial Fulfillment of the Requirements for the Degree Bachelor of Science with Honors Research Distinction in Civil Engineering at The Ohio State University

By

Mia Saurette

Undergraduate Program in Civil Engineering

The Ohio State University

2023

Thesis Committee:

Dr. Mark McCord, Advisor

Dr. Rabi Mishalani

Abstract

Origin-destination (OD) flows indicate where people come from and move to within a transportation system. For bus transit, stop-to-stop OD matrices represent the number of passengers traveling from one bus stop to another for every feasible stop pair on a bus route. Stop-to-stop OD matrices can be large and are route-specific. Their large size can present a challenge in interpreting the matrices. The route-specific nature of the matrices can limit their usefulness in planning for future route changes or interpreting changes over time that result when routes are modified.

As opposed to stop-to-stop OD matrices, zonal OD matrices aggregate passenger flows across bus routes by mapping bus stops into zones. While stop-to-stop matrices are useful in monitoring passenger flows along routes, zonal OD matrices are more fundamental in representing the geography of passenger flows because they do not rely on a specific route and instead focus on movements between geographic areas. Because there are fewer zones than stops, the zonal matrices have smaller dimensions. For these reasons, zonal OD matrices can be easier to use than stop-to-stop OD matrices in representing general demand of transit passengers and in observing patterns and spatial changes over time.

The Ohio State University's (OSU's) Campus Transit Laboratory (CTL) has been estimating stop-to-stop OD matrices from automatic passenger counter (APC) data from Campus Area Bus System (CABS) buses for many years. They deliver these estimated matrices to OSU's Transportation and Traffic Management office (TTM) on a monthly basis for TTM's general monitoring and ongoing planning. Recently, CTL has also begun estimating and delivering monthly zonal OD matrices along with the stop-to-stop matrices. When considering estimated matrices, there will be differences from one month to another. Such differences can be slight, resulting from real but uninteresting variability in passenger flows

or from imprecision in the estimates. However, differences can also be large and indicative of important changes in the spatial patterns of passenger flows. Therefore, it would be useful to have an automatic way to indicate when noteworthy changes occur in the matrices. Being able to automatically monitor changes in estimated zonal OD matrices would be of interest to TTM and to any transit agency that receives OD estimates on a regular basis.

In this thesis, a scalar metric was developed to allow comparisons between pairs of OD matrices in order to identify matrices that are similar over time, recurring differences in the matrices, and singular changes in the matrices. The metric was applied to pairs of 240 empirically estimated zonal OD matrices or aggregations of these matrices. The 240 matrices represent flows of passengers using CABS buses during four time-of-day (TOD) periods for each month between 01/2018 and 12/2022. This empirical application allowed an assessment of the metric's ability to detect noteworthy changes among spatial patterns in different zonal OD matrices. The application of the metric to the historical matrices also allowed for investigation and interpretation of similarities and changes in bus passenger flow patterns on OSU's campus over time.

The empirical results indicate that the metric is able to detect important changes in spatial flow patterns as well as periods of similarities in the patterns. Changes were indicated between matrices representing flow patterns in academic year months and matrices representing flow patterns in summer months. The metric was then used to identify groups of months in one year with similar flow patterns. Analysis of these monthly groups over the years showed that some stability in spatial patterns was maintained through time. However, there were large differences between matrices obtained before the impact of the COVID-19 pandemic on the OSU campus ("pre-lockdown" matrices) and matrices obtained during the period when OSU implemented important policy changes in response to the pandemic ("during-lockdown" matrices). Differences between the during-lockdown matrices and "post-lockdown" matrices were also large, while differences among pre-lockdown matrices were generally small. Differences between pre-lockdown and post-lockdown matrices indicated that post-lockdown spatial patterns are closer to pre-lockdown patterns than to during-lockdown patterns. This could reflect that conditions are gradually returning to pre-lockdown conditions. Alternatively, it could indicate a lasting structural change from both pre-lockdown and post-lockdown spatial flow patterns on the OSU campus.

The ability of the metric to represent changes in spatial flow patterns motivates its use for investigating the effects of specific changes in bus service on zonal passenger bus demand. The empirical results also motivate developing an additional measure to automatically identify noteworthy changes in zone pairs when large differences in the overall matrices are determined.

Dedication

To public transit users everywhere: enjoy the ride.

## Acknowledgements

Firstly, I would like to express gratitude to my thesis advisor Dr. Mark McCord whose support and guidance have made this project possible. Dr. McCord has been a mentor to me for the past two years and has played a crucial role in my success as an undergraduate researcher at The Ohio State University. I would also like to thank Dr. Rabi Mishalani for his support and advice as a member of my thesis committee.

I gratefully acknowledge The Ohio State University (OSU) Campus Transit Laboratory (CTL) for providing the contextual setting that led to the concepts developed in this study and to former graduate student Diego Galdino who, with CTL directors Drs. Mark McCord and Rabi Mishalani, provided origin-destination matrices used as input to the empirical study.

I also recognize OSU's Transportation and Traffic Management office for its financial and data support of the CTL and thank OSU's College of Engineering for awarding a scholarship for the completion of this honors undergraduate thesis.

Finally, I would like to acknowledge my parents, Patricia and David, who have always expressed confidence in my academic endeavors, along with my sisters and friends. And a special thanks to Sam, whose moral support and encouragement mean so much to me.

# Vita

2019 to 2023 ……………………………………….. B.S. in Civil Engineering, The Ohio State University

## Field of Study

Major Field: Civil Engineering

Table of Contents

List of Tables

List of Figures

# Chapter 1: Introduction

## 1.1. Background and Motivation

Origin-destination (OD) passenger flow matrices summarize where people come from and where they go to, representing the spatial patterns of passenger flow. This information is essential to designing and operating any mode of transportation or multimodal system efficiently (Horowitz et al., 2014; Meyer & Miller, 2001). For bus transit systems, OD matrices typically summarize the numbers of bus passengers traveling between stop pairs on individual bus routes (McCord et al., 2010). These are called stop-to-stop OD matrices. The spatial patterns of passenger flows are summarized in OD matrices for various homogeneous periods, such as weekdays or weekends, months or seasons, or times of special events. Since the directions of flow are usually opposite at different times of the day—for example, toward attractions such as the workplace in the morning and away from them in the evening—time-of-day (TOD) periods are important considerations when determining OD matrices (Ji et al., 2011). Bus service is adjusted by time of day, in part, to adapt to these different spatial patterns.

Because OD matrices provide passenger flows for all feasible stop-to-stop pairs, stop-to-stop matrices can often be very large and, therefore, difficult to understand in terms of important bus passenger movements. A stop-to-stop OD matrix is determined for a distinct route because different bus routes contain different sets of stops, even if there is some overlap with other routes. This limits their usefulness in planning for future route changes or interpreting changes over time. "Zonal" OD matrices aggregate passenger flows across bus routes (Reinhold, 2013). They represent the number of passengers traveling between geographic areas or zones. Because zonal OD matrices aggregate flows across bus routes, they can be easier to use in representing general demand of transit passengers and in observing patterns and spatial changes in historical data over time.

Zonal matrices can be determined from stop-to-stop OD matrices. In zonal matrices, stops are mapped to geographic zones, and the passenger movements between the zones are determined from the stop-to-stop OD flows and the stop-to-zone mapping. Zonal OD matrices can aid in visualizing passenger flows by summarizing stop-to-stop matrices into zones of interest to researchers and engineers. Details of this process are described in Section 2.1.

## 1.2. Research Question and Scope

When considering empirically determined matrices, there will be differences in spatial patterns over time. Such differences can be slight, resulting from real but uninteresting variability in passenger flows or from imprecision in matrix estimation. Therefore, it would be useful to have an automatic way to indicate when noteworthy changes occur in matrices over time. Developing metrics to monitor spatial changes in estimated zonal OD matrices will be of interest to transit agencies that use estimated OD matrices on a regular basis.

This thesis seeks to develop a metric to monitor spatial patterns in zonal OD matrices that identifies homogenous patterns, recurring differences, and singular changes over time. The metric is applied to empirical zonal OD matrices determined for travel on The Ohio State University's (OSU's) Campus Area Bus System (CABS). Comparisons of metric values to changes in spatial patterns expected from knowledge of campus bus passenger flows allowed for validation of its ability to detect noteworthy changes. In addition, application to these empirical zonal OD matrices allowed for an investigation and interpretation of bus passenger flow patterns on OSU's campus over time.

## 1.3. Thesis Overview

This thesis is organized into four chapters. In Chapter 1, the background, motivation, and objectives of the thesis are presented. In Chapter 2, the process for developing zonal origin-destination matrices, the notation used throughout the thesis, and the scalar metric used to depict differences in spatial patterns are presented. In Chapter 3, the empirical analyses and results are presented. In the first section of Chapter 3, the metric is used to compare matrices from two adjacent months for all of the historical matrices to assess the metric's ability to detect expected changes. After validating the metric's ability to perform as expected, the subsequent sections in Chapter 3 are devoted to application of the metric to investigate and interpret interesting changes and similarities in historical bus passenger flow patterns on the OSU campus over a five-year period. In the second section, the metric is used for comparisons between all pairs of monthly matrices within a one-year period to create homogenous groups of months with similar spatial flow patterns. In the third section, the groups of months are applied across the years of historical data to detect similarities and changes in passenger spatial patterns over time. In Chapter 4, the findings from this thesis are summarized and recommendations for future research are made.

# Chapter 2: Metric to Compare Zonal Origin-Destination Matrices

## 2.1. Developing Zonal Origin-Destination Matrices

The Ohio State University (OSU) Campus Transit Laboratory (CTL) uses data from the Campus Area Bus System (CABS) that is collected through automatic passenger counters (APCs) installed by OSU's Transportation and Traffic Management office (TTM). APCs count the number of passengers boarding and alighting at each bus stop. CTL uses these data as inputs to estimate origin-destination (OD) flows between bus stop pairs by route, month, and time-of-day (TOD) period for the campus area. These stop-to-stop matrices indicate the number of passengers traveling from each stop to all other stops on the route during the month and TOD period. To develop the stop-to-stop matrices, the iterative proportional fitting (IPF) method is applied (Ji et al., 2014; McCord et al., 2010). This method is also known as biproportional fitting and has been used for several applications in the past (Deming & Stephan, 1940; Kruithof, n.d.).

To develop bus passenger OD matrices, the IPF method requires as input the numbers of passengers boarding and alighting at each stop, along with a seed or base matrix. The boarding and alighting volumes can be obtained from the APC data. The base or seed matrix can be considered an initial "guess" at the spatial distribution of the boarding-stop-to-alighting-stop flows, as represented by the matrix. In the absence of historical data, a null matrix may be used. A null matrix is one in which the total passenger volume for the matrix is distributed evenly among the feasible cells. A feasible cell ($i$,$j$) is one for which travel from stop $i$ to stop $j$ is considered reasonable. For example, if stop 3 is followed by stop 4 on a bus route, it is unrealistic to assume passengers would travel from stop 4 to stop 3, making cell (4,3) an infeasible cell. Stop-to-stop OD pairs that are not feasible are assigned values of zero in the seed matrix. Assigned values of zero in the seed matrix are called “structural zeroes.” The IPF method applies a series of multiplicative factors to the base or seed matrix, so structural zeroes in the seed matrix remain zeroes in the estimated matrix because any factor multiplied by zero is zero.

CTL has been providing stop-to-stop matrices to OSU’s Transportation and Traffic Management office (TTM) on a monthly basis for several years. Figure 2.1.1 shows the stop-to-stop OD matrix provided to TTM for the Campus Loop North (CLN) route in February 2022 for the 7-11AM time-of-day (TOD) period. In this matrix, there are thirteen bus stops, which correspond to the thirteen physical stops listed in Table 2.1.1. The locations of the stops are shown in Figure 2.1.2. The stops represented in the rows of the matrices are considered “boarding stops.” The stops represented in the columns of the matrices are considered “destination stops.” Stops 1 through 13 in the columns are the same as stops 1 through 13 in the rows. Stops 14 and 15 in the columns correspond to repetition of stops 1 and 2, respectively. These repeated stops account for “carry-over” movements where passengers boarding at stops with higher numbers stay on the bus after stop 13 (the assumed terminal) to alight at stops with lower numbers (Chen, 2020). For example, passengers traveling from Herrick Transit Hub (stop 10) to Buckeye Lot Loop (stop 2) are counted in cell (10, 15) because stop 15, as well as stop 2, corresponds to Buckeye Lot Loop.

To illustrate the numerical representations in the matrix, consider the entry of 60 in cell (5, 9). This value indicates that 60 passengers traveled from stop 5 (Knowlton Hall) to stop 9 (Honors House) on the CLN bus route in February 2022 during the 7-11AM TOD period.

| | | Destination | | | | | | | | | | | | | | |
|---|---|---|---|---|---|---|---|---|---|---|---|---|---|---|---|---|
| | | 1 | 2 | 3 | 4 | 5 | 6 | 7 | 8 | 9 | 10 | 11 | 12 | 13 | 14 | 15 | |
| Origin | 1 | | 55 | 22 | 5 | 180 | 99 | 53 | 63 | 21 | 16 | 3 | | | | | 516 |
| | 2 | | | 329 | 74 | 3409 | 1653 | 872 | 852 | 350 | 259 | 64 | | | | | 7862 |
| | 3 | | | | 8 | 302 | 188 | 78 | 109 | 40 | 25 | 6 | | | | | 757 |
| | 4 | | | | | 212 | 113 | 59 | 74 | 27 | 21 | 5 | | | | | 512 |
| | 5 | | | | | | 227 | 119 | 178 | 60 | 44 | 9 | 3 | 12 | 2 | 20 | 674 |
| | 6 | | | | | | | 379 | 564 | 242 | 172 | 37 | 11 | 49 | 9 | 53 | 1516 |
| | 7 | | | | | | | | 324 | 150 | 118 | 24 | 7 | 31 | 5 | 38 | 698 |
| | 8 | | | | | | | | | 343 | 336 | 77 | 17 | 100 | 14 | 84 | 971 |
| | 9 | | | | | | | | | | 90 | 23 | 12 | 53 | 17 | 37 | 231 |
| | 10 | | | | | | | | | | | 86 | 36 | 112 | 36 | 208 | 478 |
| | 11 | | | | | | | | | | | | 30 | 54 | 9 | 40 | 133 |
| | 12 | | | | | | | | | | | | | 59 | 12 | 43 | 114 |
| | 13 | | | | | | | | | | | | | | 8 | 48 | 57 |
| | | 0 | 55 | 351 | 87 | 4102 | 2281 | 1560 | 2164 | 1234 | 1081 | 335 | 115 | 470 | 112 | 572 | 14518 |

*Figure 2.1.1: Stop-to-stop OD matrix for Campus Loop North (CLN) route, February 2022, 7-11AM TOD period*

*Table 2.1.1: List of Campus Loop North bus route stops*

| Stop No. | Name |
|---|---|
| 1 | Fred Taylor and Irving Schottenstein Drive |
| 2 | Buckeye Lot Loop |
| 3 | Midwest Campus (EB) |
| 4 | St. John Arena (EB) |
| 5 | Knowlton Hall |
| 6 | Fontana Lab |
| 7 | Stillman Hall |
| 8 | Ohio Union (SB) |
| 9 | Honors House |
| 10 | Herrick Transit Hub |
| 11 | Mid Towers |
| 12 | St. John Arena (WB) |
| 13 | Midwest Campus (WB) |

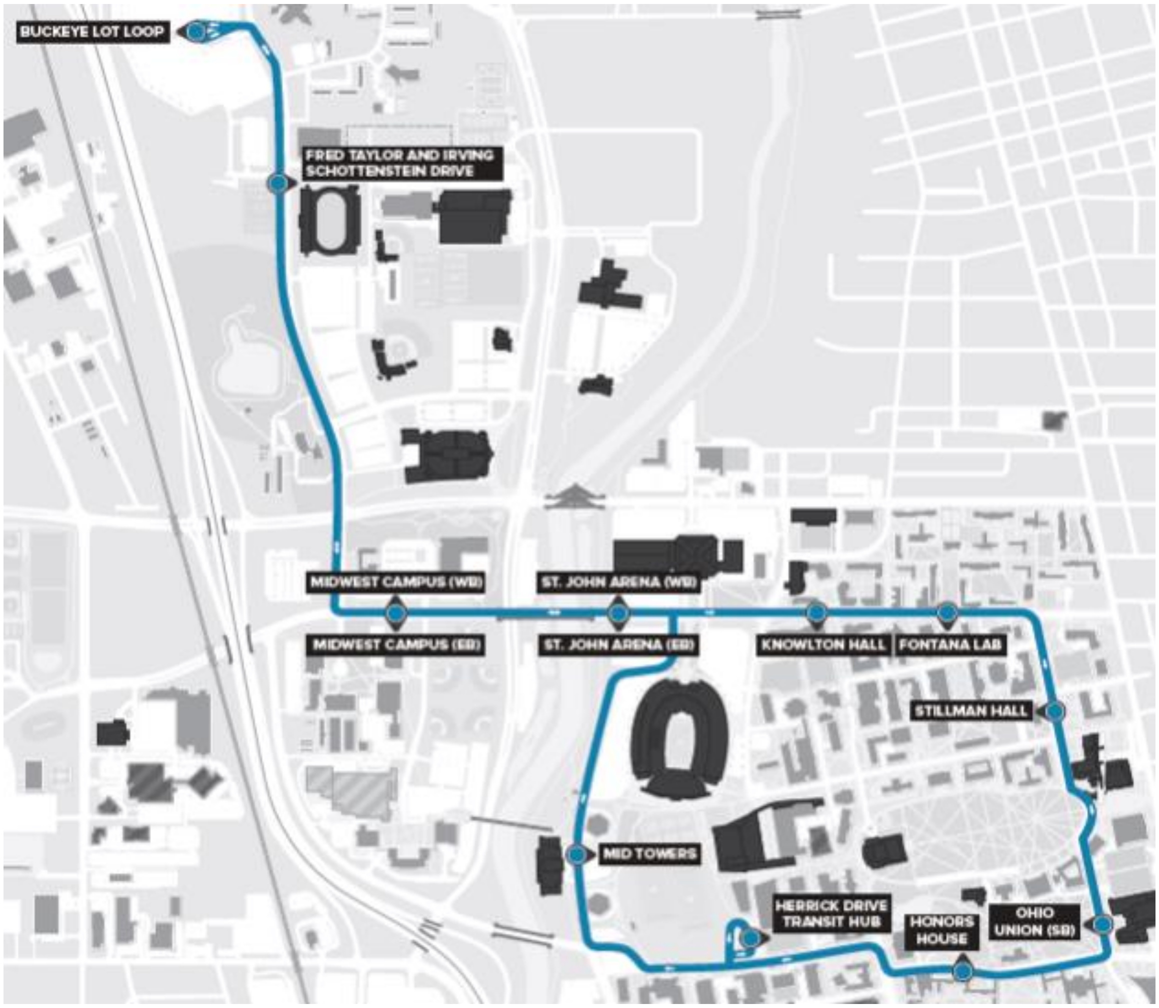


*Figure 2.1.2: Map of Campus Loop North bus route (obtained from monthly reports to the Transportation and Traffic Management office)*

A stop-to-stop OD matrix is produced using the IPF method for every bus trip on the route, and the monthly time-of-day matrix for the month is determined by adding these trip-level matrices. In this way, the matrix shown in Figure 2.1.1 is determined by adding the OD matrices determined for every bus trip within the 7-11AM TOD period during February 2022.

The single matrix shown in Figure 2.1.1 is for one route (Campus Loop North) during one month (February) over one time-of-day period (7-11AM). CTL estimates and delivers stop-to-stop OD matrices for multiple routes and four TOD periods and has recently added reports with hourly matrices. TTM uses the monthly stop-to-stop matrices for the various routes provided by CTL in their planning practices.

Stop-to-stop matrices are used to assess route performance and volumes on specific routes. Though useful, their large dimension can make them difficult to understand. Stop-to-stop matrices are also route-specific, which can limit their usefulness in planning for future route changes or interpreting changes over time that result when routes are changed. Service is often planned in terms of how many passengers are traveling from one area to another. Therefore, it is of interest to determine how many people are traveling between geographic areas. Zonal OD matrices summarize passenger movements between pairs of geographic zones regardless of bus route or stop (Reinhold, 2013).

Zonal OD matrices are created from stop-to-stop matrices by defining geographic zones, mapping stops into the zones, and adding the values in the cells for stop pairs based on their respective zones. To illustrate, consider Figures 2.1.3, 2.1.4, and 2.1.5, which show the respective stop-to-stop matrices for Campus Loop North (CLN), Campus Loop South (CLS), and West Campus (WC) in February 2022 during the 11AM-3PM TOD period. $S^{R}(i,j)$ represents the passenger volume on bus route R from stop *i* to stop *j*. For example, in Figure 2.1.3, $S^{CLN}(4,8)$ equals 55 passengers.

Assume that some geographic "zone 5" has been defined that includes CLN stops 4, 5, 6, 7, and 12; CLS stops 4, 9, 10, 11, and 12; and WC stops 8, 9, 10, 11, and 17. Another geographic "zone 7" includes CLN stop 8, CLS stop 8, and WC stop 12. Maps for the CLS and WC routes are provided in Figures 2.1.6 and 2.1.7 to show how their stops are mapped into zones, and lists of stops are presented in Tables 2.1.2 and 2.1.3. To determine the number of passengers traveling from zone 5 to zone 7, the stops from the three routes that are included in zones 5 and 7 are shaded in Figures 2.1.3, 2.1.4, and 2.1.5, with zone 5 shaded yellow in the row headers (boarding) and zone 7 shaded blue in the column headers (alighting). Row headers represent the stops as origins, while the column headers represent the stops as destinations. The row headers for stops in zone 5 are shaded yellow because passengers are leaving from zone 5. The column headers for stops in zone 7 are shaded blue because passengers are going to zone 7.

To determine how many passengers are traveling from zone 5 to zone 7, the numbers of passengers traveling from any stop within zone 5 to any stop within zone 7 for any route are summed.

(Note that some of the stop-to-stop pairs are cells containing structural zeroes, which are shaded gray.) Z($i$,$j$) represents the number of passengers traveling from zone $i$ to zone $j$. Thus, the stop-to-stop matrix cells used to calculate Z(5,7) are those that include passengers traveling via feasible OD pairs from a stop in zone 5 to a stop in zone 7.

$$
\begin{aligned}
Z(5,7) = {} & S^{CLN}(4,8) + S^{CLN}(5,8) + S^{CLN}(6,8) + S^{CLN}(7,8) + S^{CLN}(12,8) + S^{CLS}(4,8) + S^{CLS}(9,8) \\
& + S^{CLS}(10,8) + S^{CLS}(11,8) + S^{CLS}(12,8) + S^{WC}(8,12) + S^{WC}(9,12) + S^{WC}(10,12) \\
& + S^{WC}(11,12) + S^{WC}(17,12) \\
& = 55 + 429 + 1392 + 600 + 0 + 36 + 0 + 0 + 0 + 0 + 34 + 376 + 1056 + 475 + 0 \\
& = 4453
\end{aligned}
$$

To visualize this summation, the included matrix cells are shaded in red in Figures 2.1.3, 2.1.4, and 2.1.5. The sum calculated above is the number of passengers who traveled from zone 5 to zone 7 in February 2022 during the 11AM-3PM TOD period. This process is repeated for every pair of zones containing realistic stop-to-stop OD pairs.

| | | Destination | | | | | | | | | | | | | | | |
|---|---|---|---|---|---|---|---|---|---|---|---|---|---|---|---|---|---|
| | | 1 | 2 | 3 | 4 | 5 | 6 | 7 | 8 | 9 | 10 | 11 | 12 | 13 | 14 | 15 | |
| Origin | 1 | | 95 | 9 | 5 | 69 | 47 | 11 | 35 | 11 | 6 | 3 | | | | | 291 |
| | 2 | | | 140 | 33 | 1370 | 796 | 283 | 618 | 200 | 108 | 45 | | | | | 3592 |
| | 3 | | | | 29 | 666 | 604 | 158 | 412 | 121 | 59 | 28 | | | | | 2077 |
| | 4 | | | | | 101 | 72 | 21 | 55 | 18 | 11 | 5 | | | | | 281 |
| | 5 | | | | | | 432 | 147 | 429 | 131 | 67 | 29 | 10 | 15 | 6 | 62 | 1329 |
| | 6 | | | | | | | 432 | 1392 | 470 | 253 | 101 | 33 | 53 | 19 | 189 | 2942 |
| | 7 | | | | | | | | 600 | 206 | 115 | 41 | 17 | 24 | 8 | 94 | 1103 |
| | 8 | | | | | | | | | 551 | 358 | 137 | 52 | 93 | 24 | 282 | 1497 |
| | 9 | | | | | | | | | | 162 | 66 | 29 | 41 | 19 | 160 | 477 |
| | 10 | | | | | | | | | | | 265 | 143 | 249 | 84 | 854 | 1595 |
| | 11 | | | | | | | | | | | | 32 | 49 | 11 | 120 | 211 |
| | 12 | | | | | | | | | | | | | 24 | 17 | 86 | 126 |
| | 13 | | | | | | | | | | | | | | 21 | 185 | 206 |
| | | 0 | 95 | 150 | 67 | 2205 | 1950 | 1051 | 3541 | 1708 | 1138 | 718 | 316 | 549 | 208 | 2032 | 15728 |

*Figure 2.1.3: Stop-to-stop OD matrix for CLN route, February 2022, 11AM-3PM TOD period*

| Origin \ Destination | 1 | 2 | 3 | 4 | 5 | 6 | 7 | 8 | 9 | 10 | 11 | 12 | 13 | 14 | 15 | |
|---|---|---|---|---|---|---|---|---|---|---|---|---|---|---|---|---|
| 1 | | 95 | 9 | 5 | 6 | 38 | 13 | 13 | 6 | 10 | 4 | | | | | 198 |
| 2 | | | 117 | 70 | 69 | 534 | 114 | 152 | 85 | 103 | 60 | | | | | 1303 |
| 3 | | | | 69 | 68 | 376 | 157 | 172 | 94 | 104 | 58 | | | | | 1099 |
| 4 | | | | | 22 | 109 | 25 | 36 | 20 | 27 | 13 | | | | | 252 |
| 5 | | | | | | 222 | 100 | 137 | 77 | 96 | 44 | 8 | 32 | 5 | 34 | 755 |
| 6 | | | | | | | 284 | 421 | 261 | 332 | 170 | 31 | 103 | 21 | 140 | 1763 |
| 7 | | | | | | | | 566 | 444 | 587 | 322 | 51 | 197 | 32 | 228 | 2428 |
| 8 | | | | | | | | | 993 | 1322 | 716 | 120 | 480 | 74 | 513 | 4218 |
| 9 | | | | | | | | | | 352 | 201 | 40 | 158 | 21 | 190 | 962 |
| 10 | | | | | | | | | | | 616 | 117 | 536 | 81 | 533 | 1882 |
| 11 | | | | | | | | | | | | 173 | 731 | 112 | 931 | 1946 |
| 12 | | | | | | | | | | | | | 34 | 6 | 44 | 84 |
| 13 | | | | | | | | | | | | | | 16 | 116 | 132 |
| | 0 | 95 | 126 | 143 | 165 | 1279 | 694 | 1497 | 1979 | 2933 | 2204 | 540 | 2271 | 367 | 2728 | 17022 |

*Figure 2.1.4: Stop-to-stop OD matrix for CLS route, February 2022, 11AM-3PM TOD period*

| Origin \ Destination | 1 | 2 | 3 | 4 | 5 | 6 | 7 | 8 | 9 | 10 | 11 | 12 | 13 | 14 | 15 | 16 | 17 | 18 | 19 | 20 | 21 | 22 | 23 | 24 | |
|---|---|---|---|---|---|---|---|---|---|---|---|---|---|---|---|---|---|---|---|---|---|---|---|---|---|
| 1 | | 57 | 3 | 9 | 73 | 2 | 10 | 4 | 48 | 38 | 14 | 26 | 12 | 10 | 5 | 3 | | | | | | | | | 313 |
| 2 | | | 11 | 50 | 305 | 9 | 59 | 16 | 281 | 167 | 62 | 118 | 46 | 48 | 21 | 14 | | | | | | | | | 1206 |
| 3 | | | | 3 | 29 | 0 | 6 | 2 | 32 | 22 | 6 | 14 | 4 | 4 | 2 | 1 | | | | | | | | | 126 |
| 4 | | | | | 106 | 2 | 21 | 5 | 78 | 54 | 15 | 34 | 15 | 14 | 6 | 4 | | | | | | | | | 354 |
| 5 | | | | | | 51 | 128 | 50 | 661 | 432 | 136 | 294 | 116 | 105 | 42 | 33 | | | | | | | | | 2048 |
| 6 | | | | | | | 11 | 7 | 53 | 49 | 12 | 26 | 10 | 12 | 3 | 4 | | | | | | | | | 187 |
| 7 | | | | | | | | 36 | 495 | 431 | 114 | 291 | 113 | 83 | 37 | 32 | | | | | | | | | 1633 |
| 8 | | | | | | | | | 64 | 49 | 15 | 34 | 12 | 12 | 5 | 4 | | | | | | | | | 195 |
| 9 | | | | | | | | | | 436 | 136 | 376 | 148 | 114 | 51 | 42 | 13 | 34 | 18 | 69 | 2 | 10 | 91 | 3 | 1541 |
| 10 | | | | | | | | | | | 393 | 1056 | 417 | 356 | 171 | 119 | 36 | 99 | 46 | 157 | 7 | 27 | 215 | 8 | 3105 |
| 11 | | | | | | | | | | | | 475 | 187 | 184 | 78 | 53 | 16 | 52 | 20 | 82 | 3 | 13 | 111 | 4 | 1277 |
| 12 | | | | | | | | | | | | | 338 | 299 | 160 | 117 | 38 | 117 | 40 | 142 | 7 | 26 | 197 | 10 | 1493 |
| 13 | | | | | | | | | | | | | | 99 | 54 | 41 | 14 | 51 | 14 | 41 | 2 | 9 | 63 | 3 | 391 |
| 14 | | | | | | | | | | | | | | | 111 | 91 | 36 | 96 | 33 | 100 | 4 | 17 | 144 | 6 | 639 |
| 15 | | | | | | | | | | | | | | | | 118 | 54 | 125 | 43 | 160 | 8 | 30 | 224 | 9 | 769 |
| 16 | | | | | | | | | | | | | | | | | 16 | 31 | 13 | 37 | 2 | 8 | 56 | 1 | 163 |
| 17 | | | | | | | | | | | | | | | | | | 127 | 50 | 189 | 7 | 35 | 250 | 8 | 666 |
| 18 | | | | | | | | | | | | | | | | | | | 48 | 158 | 7 | 27 | 185 | 8 | 432 |
| | 0 | 57 | 14 | 61 | 513 | 64 | 237 | 120 | 1713 | 1679 | 903 | 2744 | 1417 | 1339 | 746 | 676 | 222 | 731 | 325 | 1134 | 49 | 201 | 1537 | 59 | 16539 |

*Figure 2.1.5: Stop-to-stop OD matrix for WC route, February 2022, 11AM-3PM TOD period*

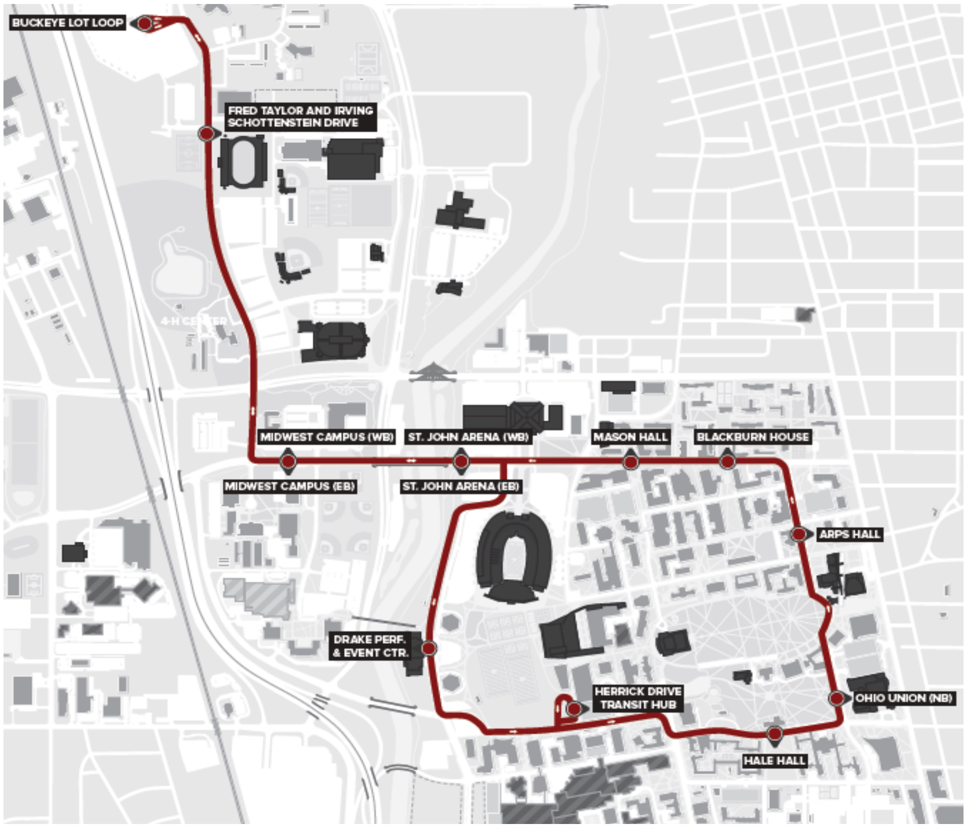


*Figure 2.1.6: Map of Campus Loop South bus route (obtained from monthly reports to the Transportation and Traffic Management office)*

*Table 2.1.2: List of Campus Loop South bus route stops*

| Stop No. | Name |
|---|---|
| 1 | Fred Taylor and Irving Schottenstein Drive |
| 2 | Buckeye Lot Loop |
| 3 | Midwest Campus (EB) |
| 4 | St. John Arena (EB) |
| 5 | Drake Center |
| 6 | Herrick Transit Hub |
| 7 | Hale Hall |
| 8 | Ohio Union (NB) |
| 9 | Arps Hall |
| 10 | Blackburn House |
| 11 | Mason Hall |
| 12 | St. John Arena (WB) |
| 13 | Midwest Campus (WB) |

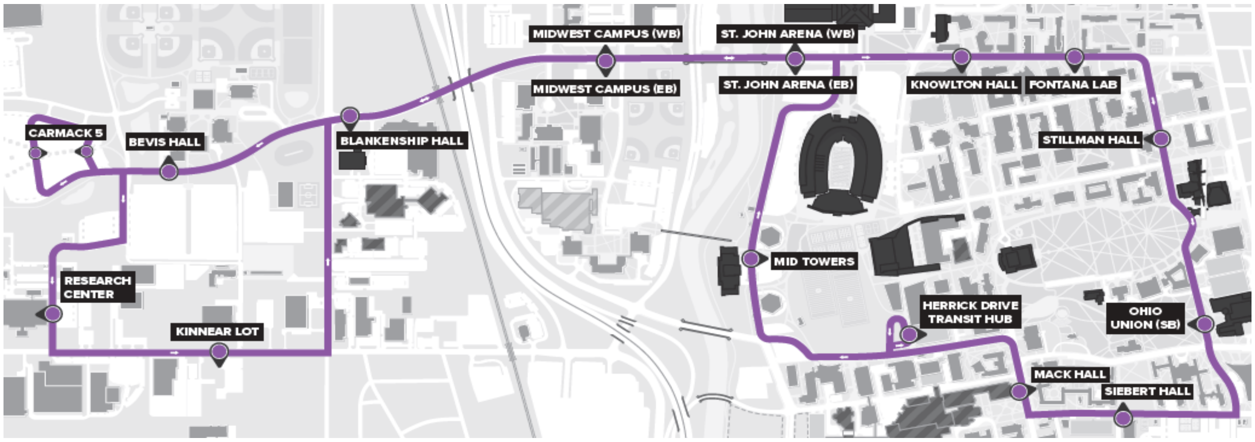


*Figure 2.1.7: Map of West Campus bus route (obtained from monthly reports to the Transportation and Traffic Management office)*

*Table 2.1.3: List of West Campus bus route stops*

| Stop No. | Name |
|---|---|
| 1 | Bevis Hall |
| 2 | Carmack 5A |
| 3 | Carmack 5B |
| 4 | Research Center |
| 5 | Kinnear Road Lot |
| 6 | Blankenship Hall |
| 7 | Midwest Campus (EB) |
| 8 | St. John Arena (EB) |
| 9 | Knowlton Hall |
| 10 | Fontana Lab |
| 11 | Stillman Hall |
| 12 | Ohio Union (SB) |
| 13 | Siebert Hall |
| 14 | Mack Hall |
| 15 | Herrick Transit Hub |
| 16 | Mid Towers |
| 17 | St. John Arena (WB) |
| 18 | Midwest Campus (WB) |

Through collaboration between TTM and CTL, mutually exclusive and collectively exhaustive geographic zones were determined that encompass the campus region served by several CABS routes. Figure 2.1.8 provides a map of the established zones. Table 2.1.4 gives the names/locations, numbers, and colors of the zones. Table 2.1.5 lists which stops belong to which zones for each route considered in this thesis that was running during February 2022. Different configurations of bus routes and stops that may have been used over the time period studied in this thesis are automatically accounted for through the use of software that maps stops into zones when producing zonal OD matrices (see pg. 14).

As shown in Figure 2.1.8, zone 1 encompasses west campus, which includes parts of the agricultural campus as well as research centers and clinics. Zone 2 encompasses midwest campus, which includes some recreational facilities and the veterinary school. Zone 3 includes Buckeye Lot parking and the athletic campus. Zone 4 includes the Towers (student housing to the west of main campus). Zones 5 and 6 encompass north and south campus, respectively, which include academic buildings, residence halls, libraries, student recreational facilities, and dining halls. Zone 7 includes the Ohio Union. Capturing movements to and from these established zones are likely to reflect important patterns.

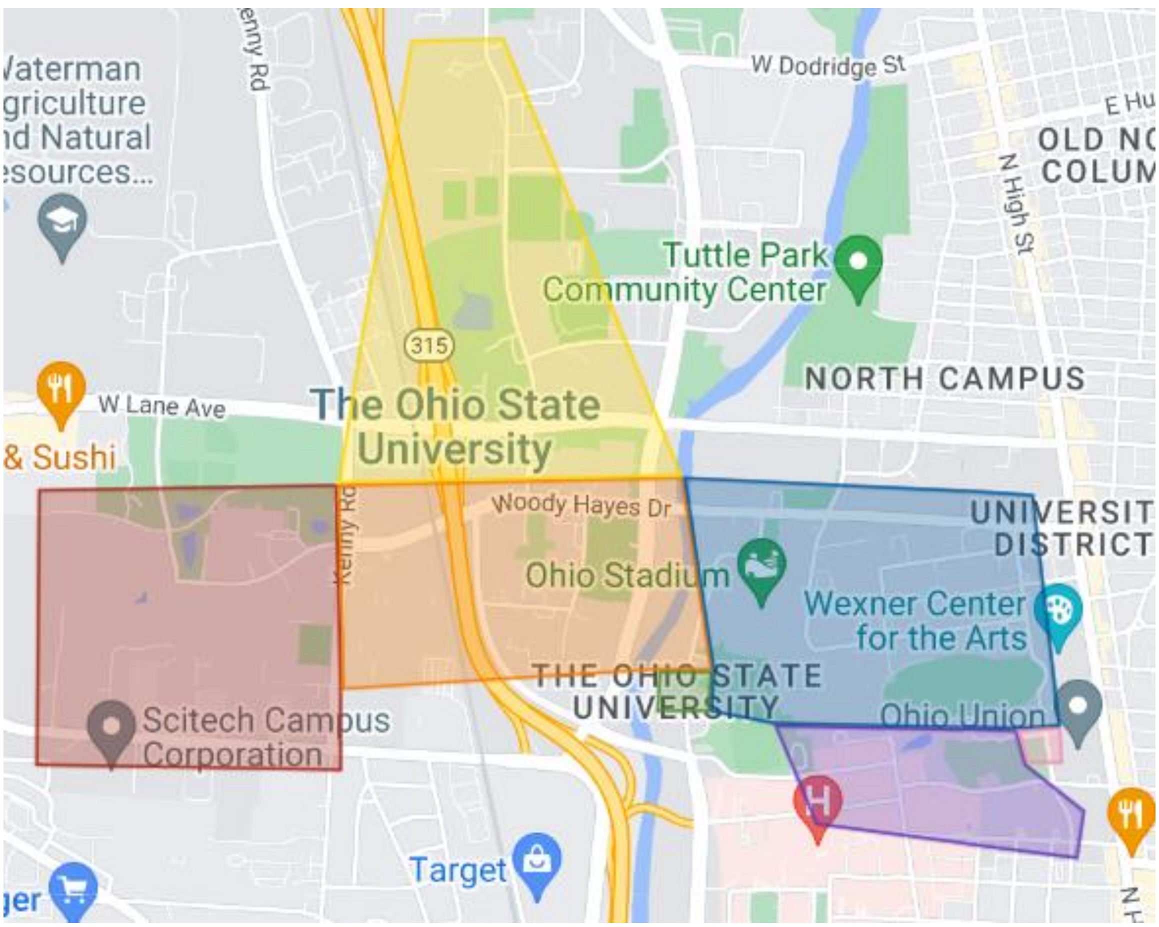


*Figure 2.1.8: Map of zones for campus area*

*Table 2.1.4: Zones for campus area*

| Zone | Color | Name |
|---|---|---|
| 1 | Red | West Campus |
| 2 | Orange | Midwest Campus |
| 3 | Yellow | Buckeye Lot Loop and Athletic Campus |
| 4 | Green | Towers |
| 5 | Blue | North Campus |
| 6 | Purple | South Campus |
| 7 | Pink | Ohio Union |

*Table 2.1.5: Stop-to-zone mapping for CLN, CLS, and WC for February 2022*

| Zone | CLN Stops | CLS Stops | WC Stops |
|---|---|---|---|
| 1 | | | 1, 2, 3, 4, 5, 19, 20, 21, 22, 23 |
| 2 | 3, 13 | 3, 13 | 6, 7, 18, 24 |
| 3 | 1, 2, 14, 15 | 1, 2, 14, 15 | |
| 4 | 11 | 5 | 16 |
| 5 | 4, 5, 6, 7, 12 | 4, 9, 10, 11, 12 | 8, 9, 10, 11, 17 |
| 6 | 9, 10 | 6, 7 | 13, 14, 15 |
| 7 | 8 | 8 | 12 |

The process of determining zonal OD matrices from stop-to-stop matrices, as demonstrated previously, was automated using software components developed by the CTL directors and a research engineer. This software processes APC data from the buses, applies IPF to determine route-level stop-to-stop matrices, automatically maps stops to zones given geographical input about the established zones, and aggregates the route-level OD matrices. The components have been integrated to establish an operational zonal OD estimation process. CTL provides APC data and geographical information about stops and zones. Several user inputs are required to produce the desired matrix. These inputs include the month, year, and time-of-day (TOD) period for which the matrix is being determined; whether the matrix is to be determined for weekdays or weekend days; and which bus routes to include. Maps and lists of stops for all CABS bus routes used in this thesis that were running during the period studied (01/2018 to 12/2022) are located in Appendix A. A list of which bus routes were running by month is located in Appendix B.

Additionally, zonal OD matrix determination depends on how trip-level OD matrices are aggregated into TOD periods. Such aggregation can be based on the time the bus trip departs from a terminal, on passenger boarding times, or on passenger alighting times. If trips are aggregated by departure time from the terminal, all boarding and alighting passengers on a bus that left the terminal at 10:59AM, for example, would be included in the 7-11AM TOD period, even though most of the trip and the passenger boardings and alightings would occur after 11AM. If trips are aggregated by boarding times, the time at which a passenger boards determines where that data point is sorted in terms of TOD period. Similarly, if trips are aggregated by alighting times, the time at which a passenger alights determines where that data point is sorted in terms of TOD period.

The zonal OD matrices used in this research are aggregated into TOD periods based on passenger boarding times. Matrices produced using boarding times and matrices produced using alighting times were highly correlated (correlation coefficient greater than 0.99 for all four TOD periods) (Appendix C). For this reason, either could be used. Using matrices based on passenger boarding times was chosen. The software was used by CTL to produce zonal OD matrices by passenger boarding times on weekdays during four TOD periods for each month between 01/2018 and 12/2022. For this thesis, only the beginning part of the month of August was used to determine matrices, thus excluding the part of the month during which the academic year begins.

An example of a zonal OD matrix produced using the software is shown in Figure 2.1.9. It contains passenger flows for February 2022 during the 11AM-3PM TOD period. The value of the cell shaded in red in Figure 2.1.9 is Z(5,7), which equals 4501. This means 4501 passengers traveled from zone 5 to zone 7 on the weekdays in February 2022 between 11AM and 3PM. There are four structural zeroes in the zonal OD matrix that result from the routes included and zones established. Cells (1,3) and (3,1) contain zeroes because there are no direct stop-to-stop connections between the two zones (west campus and Buckeye Lot/athletic campus) on any of the routes. Cells (4,4) and (7,7) contain zeroes because zones 4 and 7 encompass very small regions with only one stop in each direction per zone (the

Towers and Ohio Union, respectively). Passengers do not board and alight in the same zone in these cases because passengers do not get on and off at the same stop.

| | | Destination | | | | | | | |
|---|---|---|---|---|---|---|---|---|---|
| | | 1 | 2 | 3 | 4 | 5 | 6 | 7 | |
| Origin | 1 | 639 | 292 | 0 | 55 | 2167 | 456 | 501 | 4110 |
| | 2 | 412 | 19 | 356 | 133 | 3100 | 996 | 912 | 5928 |
| | 3 | 0 | 276 | 189 | 122 | 2933 | 1028 | 809 | 5357 |
| | 4 | 109 | 116 | 163 | 0 | 280 | 349 | 135 | 1154 |
| | 5 | 1378 | 2184 | 2552 | 404 | 4166 | 3153 | 4501 | 18338 |
| | 6 | 956 | 970 | 1529 | 583 | 2537 | 725 | 979 | 8280 |
| | 7 | 408 | 739 | 913 | 247 | 3248 | 1751 | 0 | 7305 |
| | | 3901 | 4596 | 5702 | 1545 | 18432 | 8458 | 7837 | 50472 |

*Figure 2.1.9: Zonal OD matrix for February 2022, 11AM-3PM TOD period*

2.2. Notation

The 240 empirical zonal OD matrices analyzed in this thesis consider sixty month-year combinations *m*. For each month-year combination, there are four TOD periods defined such that *t* = 1, 2, 3, and 4 correspond to 7-11AM, 11AM-3PM, 3-6PM, and 6-9PM, respectively. These TOD periods were selected because they are the periods established for reports to TTM. Table 2.2.6 lists the *t*-values, and Table 2.2.7 lists the sixty *m*-values that correspond to the month-year combinations used in the subsequent analysis. These combinations are numbered chronologically over several years. That is, *m* = 1, 2, 3, …, 60 correspond to 01/2018, 02/2018, 03/2018, …, 12/2022, respectively.

A zonal OD volume matrix is denoted as $\boldsymbol{V_{t,m}}$, where *t* indicates the time-of-day (TOD) period and *m* indicates the month-year combination. An element of the zonal OD volume matrix $\boldsymbol{V_{t,m}}$ is denoted as $V_{t,m}(i,j)$, which is the number of passengers traveling from zone *i* to zone *j* during TOD period *t* and month-year combination *m*. In this thesis, forty-nine OD pairs are considered in the zonal matrix with *i*- and *j*-values ranging from 1 to 7, each. As an example, the zonal OD volume matrix for 05/2022 (*m* = 53) during the 7-11AM TOD (*t* = 1), $\boldsymbol{V_{1,53}}$, is shown in Figure 2.2.10. In this example matrix, $V_{1,53}(2,5)$ equals 129, indicating that 129 passengers traveled during the 7-11AM period (*t* = 1) in 05/2022 (*m* = 53) from zone 2 (Midwest Campus, see Section 2.1) to zone 5 (North Campus, see Section 2.1). The volumes in the matrix in Figure 2.2.10 are shown rounded to the nearest whole numbers for presentation purposes, but calculations performed for analysis are conducted without rounding.

*Table 2.2.6: Time-of-day (TOD) periods indicated by* t*-values used in analysis*

| ***t*** | **TOD period** |
|---|---|
| 1 | 7-11AM |
| 2 | 11AM-3PM |
| 3 | 3-6PM |
| 4 | 6-9PM |

*Table 2.2.7: Month-year combinations indicated by* m*-values used in analysis*

| ***m*** | **MM/YYYY** | ***m*** | **MM/YYYY** | ***m*** | **MM/YYYY** | ***m*** | **MM/YYYY** | ***m*** | **MM/YYYY** |
|---|---|---|---|---|---|---|---|---|---|
| 1 | 01/2018 | 13 | 01/2019 | 25 | 01/2020 | 37 | 01/2021 | 49 | 01/2022 |
| 2 | 02/2018 | 14 | 02/2019 | 26 | 02/2020 | 38 | 02/2021 | 50 | 02/2022 |
| 3 | 03/2018 | 15 | 03/2019 | 27 | 03/2020 | 39 | 03/2021 | 51 | 03/2022 |
| 4 | 04/2018 | 16 | 04/2019 | 28 | 04/2020 | 40 | 04/2021 | 52 | 04/2022 |
| 5 | 05/2018 | 17 | 05/2019 | 29 | 05/2020 | 41 | 05/2021 | 53 | 05/2022 |
| 6 | 06/2018 | 18 | 06/2019 | 30 | 06/2020 | 42 | 06/2021 | 54 | 06/2022 |
| 7 | 07/2018 | 19 | 07/2019 | 31 | 07/2020 | 43 | 07/2021 | 55 | 07/2022 |
| 8 | 08/2018 | 20 | 08/2019 | 32 | 08/2020 | 44 | 08/2021 | 56 | 08/2022 |
| 9 | 09/2018 | 21 | 09/2019 | 33 | 09/2020 | 45 | 09/2021 | 57 | 09/2022 |
| 10 | 10/2018 | 22 | 10/2019 | 34 | 10/2020 | 46 | 10/2021 | 58 | 10/2022 |
| 11 | 11/2018 | 23 | 11/2019 | 35 | 11/2020 | 47 | 11/2021 | 59 | 11/2022 |
| 12 | 12/2018 | 24 | 12/2019 | 36 | 12/2020 | 48 | 12/2021 | 60 | 12/2022 |

| Zone OD | 1 | 2 | 3 | 4 | 5 | 6 | 7 | Total On |
|---|---|---|---|---|---|---|---|---|
| 1 | 60 | 183 | 0 | 20 | 941 | 189 | 256 | 1,649 |
| 2 | 49 | 10 | 23 | 5 | 129 | 90 | 85 | 392 |
| 3 | 0 | 234 | 10 | 87 | 944 | 846 | 340 | 2,462 |
| 4 | 10 | 7 | 11 | 0 | 17 | 17 | 20 | 82 |
| 5 | 159 | 210 | 186 | 30 | 198 | 285 | 240 | 1,308 |
| 6 | 123 | 95 | 135 | 36 | 99 | 46 | 102 | 635 |
| 7 | 131 | 189 | 118 | 46 | 237 | 235 | 0 | 956 |
| Total Off | 532 | 928 | 483 | 224 | 2,565 | 1,708 | 1,043 | 7,483 |

*Figure 2.2.10: Zonal OD volume matrix for May 2022, 7-11AM (*$\boldsymbol{V}_{\boldsymbol{1,53}}$*)*

The matrix presented in Figure 2.2.10 is a volume OD matrix, which represents the number of passengers traveling between zones for each zone pair. A volume OD matrix, $\boldsymbol{V}_{\boldsymbol{t,m}}$, can be converted to a probability OD matrix, $\boldsymbol{P_{t.m}}$ (Chen, 2020; Ji et al., 2014; Ji et al., 2015), where the value in a cell represents the likelihood that a passenger chosen randomly from all the passengers represented in the matrix traveled along the OD pair associated with the cell during the given month-year combination and TOD period. These probability matrices are useful in comparing spatial patterns because they retain the proportions of travelers from every zone to every other zone while eliminating the effect of total volume. That is, probability OD matrices can be used to effectively compare matrices with different volumes. A probability matrix corresponding to volume matrix $\boldsymbol{V_{t,m}}$ is calculated by dividing the number of passengers in each cell by the total volume of the matrix $T_{t,m}$.

$$\boldsymbol{P_{t.m}} = \frac{\boldsymbol{V_{t,m}}}{T_{t,m}} \tag{2.2.1}$$

with

$$T_{t,m} = \sum_{\forall(i,j)} V_{t,m}(i,j) \tag{2.2.2}$$

The variable $T_{t,m}$ is not bold-faced because it represents a scalar value rather than a matrix.

The zonal OD probability matrix for 05/2022 during the 7-11AM TOD period, for example, is denoted $\boldsymbol{P_{1.53}}$ and shown in Figure 2.2.11. The element of the zonal OD probability matrix denoted $P_{1,53}(2,5)$ equals 0.01727, which is the probability that a passenger drawn at random from all passengers traveling in 05/2022 during the 7-11AM TOD period traveled from zone 2 to zone 5. That is, 1.727 percent of all passengers who traveled on CABS during the period went from zone 2 (Midwest Campus, see Section 2.1) to zone 5 (North Campus, see Section 2.1).The probabilities in the matrix must sum to 1 by construction.

| Zone OD | 1 | 2 | 3 | 4 | 5 | 6 | 7 | Total On |
|---|---|---|---|---|---|---|---|---|
| 1 | 0.00801 | 0.02444 | 0 | 0.00264 | 0.12581 | 0.02531 | 0.03419 | 0.2204 |
| 2 | 0.0066 | 0.00129 | 0.00311 | 0.00071 | 0.01727 | 0.012 | 0.01134 | 0.05233 |
| 3 | 0 | 0.03127 | 0.00135 | 0.01162 | 0.12615 | 0.11306 | 0.0455 | 0.32895 |
| 4 | 0.0014 | 0.00089 | 0.00144 | 0 | 0.00223 | 0.00231 | 0.0027 | 0.01097 |
| 5 | 0.02123 | 0.02813 | 0.02487 | 0.00398 | 0.0264 | 0.03804 | 0.03213 | 0.17477 |
| 6 | 0.0164 | 0.01275 | 0.01798 | 0.00485 | 0.01318 | 0.00615 | 0.01357 | 0.08489 |
| 7 | 0.01751 | 0.02526 | 0.01576 | 0.00612 | 0.03169 | 0.03135 | 0 | 0.12769 |
| Total Off | 0.07115 | 0.12404 | 0.06451 | 0.02992 | 0.34273 | 0.22822 | 0.13944 | 1 |

*Figure 2.2.11: Zonal OD probability matrix for May 2022, 7-11AM ($\boldsymbol{P}_{1,53}$)*

## 2.3. Metric to Depict Differences in Spatial Patterns

To compare the spatial patterns represented by two probability matrices $\boldsymbol{P}_{\boldsymbol{t},\boldsymbol{m}}$ and $\boldsymbol{P}_{\boldsymbol{t}',\boldsymbol{m}'}$, the absolute value of the cell-by-cell difference between the two probability matrices is calculated to produce an "absolute difference matrix," $\boldsymbol{D}_{(\boldsymbol{t},\boldsymbol{m});(\boldsymbol{t}',\boldsymbol{m}')}$:

$$\boldsymbol{D}_{(\boldsymbol{t},\boldsymbol{m});(\boldsymbol{t}',\boldsymbol{m}')} = ABS(\boldsymbol{P}_{\boldsymbol{t},\boldsymbol{m}} - \boldsymbol{P}_{\boldsymbol{t}',\boldsymbol{m}'}) \tag{2.3.3}$$

where ABS indicates the absolute value, in this case, of the difference between the two probability matrices for each cell.

Similar to volume and probability matrices, an element of an absolute difference matrix is denoted as $D_{(t.m);(t',m')}(i,j)$. All of the cells in this absolute difference matrix are averaged to produce a scalar metric called the average difference value, *ADV*:

$$ADV_{(t,m);(t',m')} = \frac{\sum_{\forall(i,j)} D_{(t,m);(t',m')}(i,j)}{c} \tag{2.3.4}$$

where *c* is the total number of cells in the zonal OD matrix. As previously stated, there are forty-nine cells in the zonal OD matrices in this thesis, meaning *c* equals 49. The *ADV* is a scalar metric for comparing spatial patterns in zonal OD matrices. Note that *ADV* = 0 means that, on average, there is no difference between two matrices. A larger *ADV* means there are, on average, greater absolute cell-by-cell differences, which will be used to indicate greater difference in the spatial patterns of the matrices. The absolute value of the difference is taken to prevent positive and negative differences from canceling each other out.

There are four structural zeroes within the zonal OD matrices that occur in all of the matrices considered. Since they occur in all of the matrices, they have the same contribution to all *ADV*s computed for the investigated empirical comparisons.

## Chapter 3: Empirical Analysis

### 3.1. Consecutive Months Comparisons

Absolute difference matrices $\boldsymbol{D}$ (Equation 3.1.1) are determined for consecutive months from $m$ = 37 (01/2021 vs. 02/2021) to $m$ = 52 (04/2022 vs. 05/2022) for the same TOD period $t$ for all four TOD periods, $t$ = 1, 2, 3, and 4. This range of months was selected to allow a preliminary validation that the metric was producing expected results while using matrices that were available at the time of this preliminary analysis. Because consecutive months are considered, the following matrices are found:

$$\boldsymbol{D}_{(\boldsymbol{t},\boldsymbol{m+1}),(\boldsymbol{t},\boldsymbol{m})} = ABS\left(\boldsymbol{P}_{\boldsymbol{t},\boldsymbol{m+1}} - \boldsymbol{P}_{\boldsymbol{t},\boldsymbol{m}}\right), \quad m = 37, 38, \dots, 52; t = 1, 2, 3, 4 \tag{3.1.1}$$

Equation 2.3.4 is applied to the $\boldsymbol{D}$ matrices in Equation 3.1.1 to determine an *ADV* for each $\boldsymbol{D}$ matrix:

$$ADV_{(t,m+1),(t,m)} = \frac{\sum_{\forall(i,j)} D_{(t,m+1),(t,m)}(i,j)}{c}, \; m = 37, 38, \dots, 52; t = 1, 2, 3, 4 \tag{3.1.2}$$

These *ADV*s are plotted in Figure 3.1.1. The number on the x-axis represents $m$ for the data point, which is the first of the two consecutive months that are compared. (Month-year combinations corresponding to the denoted $m$ values can be found in Table 2.2.7.)

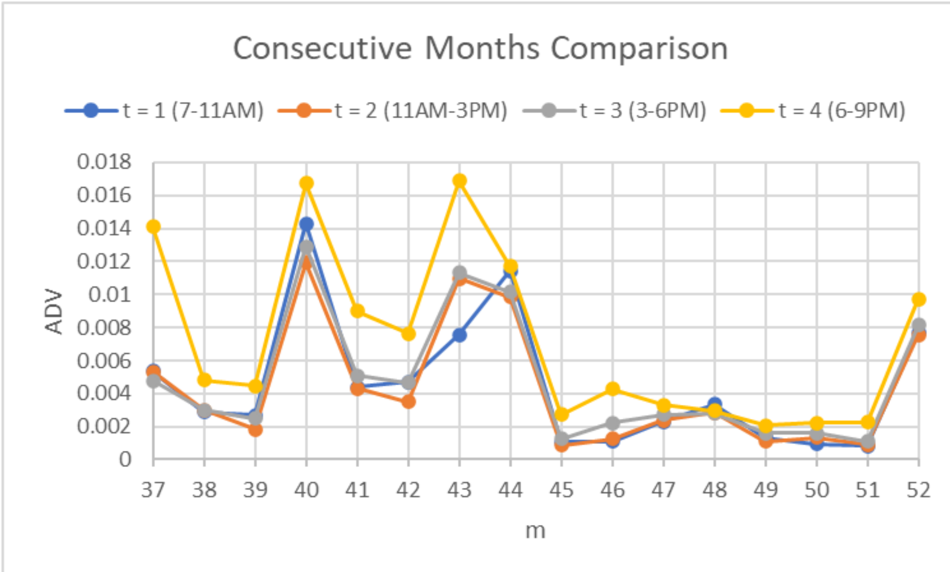


*Figure 3.1.1: Plot of consecutive month-to-month* $ADVs_{(t,m+1),(t,m)}$ *for* m *= 37, 38, …, 52 and* t *= 1, 2, 3, 4*

In Figure 3.1.1, *ADV*s that are small compared to other *ADV*s are seen across all TOD periods (*t* = 1, 2, 3, and 4) for *m* = 38 (02/2021 vs. 03/2021) and *m* = 39 (03/2021 vs. 04/2021) and from *m* = 45 (09/2021 vs. 10/2021) to *m* = 51 (03/2022 vs. 04/2022). These consistently small ADVs indicate similarity in spatial patterns between zonal OD matrices in consecutive months during the academic year 2021 to 2022, where the "academic year" consists of months September, October, November, December, January, February, March, and April. As mentioned in Section 2.1, only weekdays are used in the determination of the matrices used in this thesis. Therefore, matrices reflect when classes are in session and students, faculty, and other employees would tend to be coming to and leaving different regions of campus on a regular schedule from month to month.

In Figure 3.1.1, *ADV*s that are large compared to other *ADV*s are seen across all TOD periods at *m* = 40 (04/2021 vs. 05/2021), *m* = 43 (07/2021 vs. 08/2021), *m* = 44 (08/2021 vs. 09/2021), and *m* = 52 (04/2022 vs. 05/2022). The large *ADV*s reflect that the spatial flow patterns changed greatly from the end of the academic years (04/2021 and 04/2022) to the start of the summers (05/2021 and 05/2022) and from the end of the summer (08/2021) to the start of a new academic year (09/2021). That is, the spatial flow pattern is very different between the academic year and the “summer” period, where the “summer” period refers to the months May, June, July, and August. Recall from Section 2.1 that zonal OD matrices for the months of August were produced using only the portion of the month before the start of the academic year. At $m$ = 43 (07/2021 vs. 08/2021), there are differences between the spatial patterns among the TOD periods, most notably for the 6-9PM TOD period. Future work will aid in interpreting unexplained differences such as these (see Section 4.2). A more formal statistical analysis (e.g., hypothesis testing) of similarities and differences in *ADV*s across sets of months and TOD periods is beyond the scope of this thesis and could also be a topic for future work.

At $m$ = 41 (05/2021 vs. 06/2021) and $m$ = 42 (06/2021 vs. 07/2021), *ADV*s are smaller than peak values but larger than the small values seen when comparing matrices in consecutive months during the academic year. Because the *ADV*s for these comparisons are smaller than peak values, the *ADV* metric reflects more similarity from month-to-month during the summer than between the end of the academic year and the start of summer. Because the *ADV*s are larger than the small values seen when comparing matrices in consecutive months during the academic year, the metric reflects larger differences in flow patterns between consecutive summer months than between consecutive academic year months. This means that, according to the *ADV* metric, flow patterns are changing more from month to month during the summer than from month to month during the academic year.

The 6-9PM TOD period ($t$ = 4) departs notably from the others at $m$ = 37 (01/2021 vs. 02/2021) and from $m$ = 41 (05/2021 vs. 06/2021) to $m$ = 43 (07/2021 vs. 08/2021). Although the *ADV*s for the $t$ = 4 TOD period are generally larger than the *ADV*s for the other TOD periods, the *ADV*s still follow the same general pattern as in the other TOD periods. The $t$ = 4 TOD period generally produces matrices with low passenger volumes (fewer people using CABS buses in this TOD period than in the other TOD periods). Low passenger volumes could cause more uncertainty in estimating trip-level OD flows with the IPF method. The differences in *ADV*s for the 6-9PM TOD period may be a result of this uncertainty in estimation. It is also possible that the 6-9PM TOD period lacks the clear origins (e.g., residences and parking lots) and destinations (e.g., academic buildings) seen in earlier TOD periods during which most courses are offered. Student organizations may hold meetings on weeknights, but these are not as consistent or frequent as class schedules, which could result in zonal OD patterns that differ more from month to month in this TOD period than in earlier TOD periods.

Figure 3.1.1 shows month-to-consecutive-month comparisons (*m* vs. *m+1*) from *m* = 37 (01/2021 vs. 02/2021) to *m* = 52 (04/2022 vs. 05/2022). This allowed identification of similarities and differences in the overall OD flow patterns for consecutive months from the start of 2021 through the academic year 2021 to 2022. *ADV*s for month-to-consecutive-month comparisons (*m* vs. *m+1*) were then determined for all of the months in the data set, *m* = 1 (01/2018 vs. 02/2018) to *m* = 59 (11/2022 vs. 12/2022), for the four TOD periods (*t* = 1, 2, 3, and 4):

$$\boldsymbol{D}_{(\boldsymbol{t},\boldsymbol{m+1}),(\boldsymbol{t},\boldsymbol{m})} = ABS\big(\boldsymbol{P}_{\boldsymbol{t},\boldsymbol{m+1}} - \boldsymbol{P}_{\boldsymbol{t},\boldsymbol{m}}\big), \quad m = 1, 2, \ldots, 59; t = 1, 2, 3, 4 \tag{3.1.3}$$

$$ADV_{(t,m+1),(t,m)} = \frac{\sum_{\forall(i,j)} D_{(t,m+1),(t,m)}(i,j)}{c}, \; m = 1, 2, \ldots, 59; t = 1, 2, 3, 4 \tag{3.1.4}$$

The *ADV*s for these month-to-consecutive-month comparisons are plotted in Figure 3.1.2. The number on the x-axis again represents *m* for the data point, as defined in Table 2.2.7. The data point represents a comparison between *m* and the month immediately following it *m+1*, as shown in Equations 3.1.3 and 3.1.4.

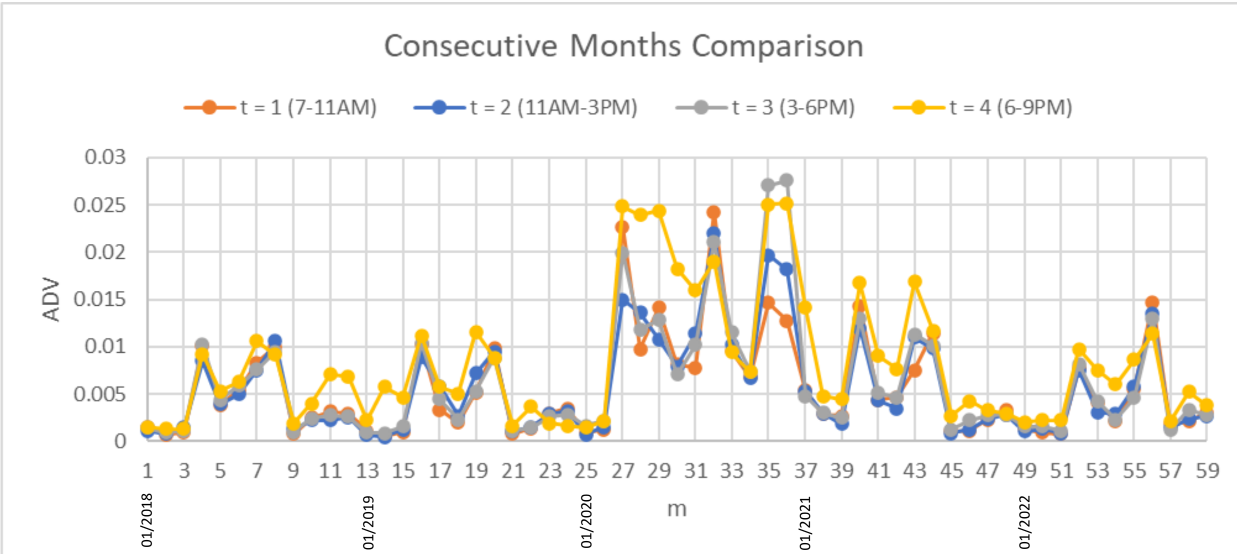

*Figure 3.1.2: Plot of consecutive month-to-month* $ADVs_{(t,m+1),(t,m)}$ *from* m *= 1 to* m *= 59 for* t *= 1, 2, 3, 4*

The patterns seen in Figure 3.1.1 generally hold in Figure 3.1.2. The largest *ADV*s occur for comparisons between matrices in the final month of the academic year and matrices in the first month of the summer and again for comparisons between matrices in the final month of the summer and matrices in the first month of a new academic year. Small *ADV*s occur consistently for comparisons between matrices in adjacent months during the academic year. *ADV*s for comparisons between matrices in adjacent summer months are lower than the largest *ADV*s but larger than *ADV*s for comparisons between matrices in adjacent months during academic years. The 6-9PM TOD period ($t$ = 4) has slightly larger *ADV*s than the other TOD periods, but the pattern for the $t$ = 4 TOD period is similar to that of the other TOD periods.

In Figure 3.1.2, there is a very large *ADV* at $m$ = 27 (03/2020 vs. 04/2020). During 03/2020, OSU administration began implementing policies in response to COVID-19 outbreaks which prevented students from returning to campus housing and in-person classes after spring break during mid-March of 2020. As a result, significantly fewer students and nonessential workers were coming to and leaving campus. However, many essential workers (maintenance, cleaning, etc.) continued coming to and leaving campus. The different impact that COVID-19 policies had on different OSU groups could result in important changes in spatial patterns, which the *ADV* metric reflects.

*ADV*s drop below the peak at $m$ = 27 (03/2020 vs. 04/2020) but remain relatively large from $m$ = 28 (04/2020 vs. 05/2020) to $m$ = 36 (12/2020 vs. 01/2021). Even though some students returned to campus at the start of the academic year 2020 to 2021, the majority of classes remained online or hybrid. For this reason, students and faculty were less likely to have established schedules that were as regular as those before the pandemic. This would be reflected in spatial flow patterns.

*ADV*s are notably smaller than peak COVID-19 *ADV*s from $m$ = 28 (04/2020 vs. 05/2020) to $m$ = 31 (07/2020 vs. 08/2020), with the exception of the 6-9PM TOD period ($t$ = 4). This period is the summer after the initial COVID-19 policies were implemented. This could indicate some similarity in spatial flow patterns from the beginning of the COVID-19 lockdown to the start of the new academic year 2020 to 2021. There is a large *ADV* at $m$ = 32 (08/2020 vs. 09/2020), which marks the end of summer and start of a new academic year in which most classes were taught online. Like non-COVID-19 years, this peak is likely due to the start of a new academic year with students returning to campus, but it is different because of online class policies and a decreased number of students living on campus that is unique to the 2020 to 2021 academic year.

There are large differences in *ADV*s among the four TOD periods at $m$ = 35 (11/2020 vs. 12/2020) and 36 (12/2020 vs. 01/2021). This could be attributed to changes in CABS routes in operation from 11/2020 to 12/2020 and from 12/2020 to 01/2021. These changes are shown in Appendix B, which lists what CABS routes analyzed in this thesis were running during each month. One route (Buckeye Loop) that was running during 11/2020 was not running during 12/2020 but was added back during 01/2021. These changes could have impacted passenger flows and caused deviation from what may otherwise have been similar spatial patterns from November through January without the route changes.

## 3.2. Homogenous Groups of Months

Figures 3.1.1 and 3.1.2 depict comparisons of spatial passenger flow patterns between zonal OD matrices for consecutive months. These comparisons allowed an identification of abrupt changes in patterns between consecutive months and of consistent patterns in consecutive months. Behavioral interpretations associated with the changes between consecutive months and periods of consistent patterns over several months presented above also helped to validate the use of the *ADV* metric to depict similarities and changes in the OD matrices through a single scalar metric. However, it is also interesting to compare similarities and differences in OD flow patterns between matrices in nonconsecutive months. Therefore, the *ADV* metric is next used to compare nonconsecutive months to identify groups of homogeneous months.

To organize the spatial OD flow patterns into homogeneous groups while limiting the number of combinations considered, *ADV*s were calculated between every pair of monthly OD matrices during the twelve-month period from $m$ = 41 (05/2021) to $m$ = 52 (04/2022) for the 11AM-3PM TOD period ($t$ = 2):

$$\boldsymbol{D}_{(\boldsymbol{t},\boldsymbol{m});(\boldsymbol{t}',\boldsymbol{m}')} = ABS(\boldsymbol{P}_{\boldsymbol{t},\boldsymbol{m}} - \boldsymbol{P}_{\boldsymbol{t}',\boldsymbol{m}'}),$$

$$m = 41\ and\ m' = 42, m = 41\ and\ m' = 43, \dots, m = 51\ and\ m' = 52; t = 2 \tag{3.2.5}$$

$$ADV_{(t,m);(t',m')} = \frac{\sum_{\forall(i,j)} D_{(t,m);(t',m')}(i,j)}{c},$$

$$m = 41\ and\ m' = 42, m = 41\ and\ m' = 43, \dots, m = 51\ and\ m' = 52; t = 2 \tag{3.2.6}$$

Figure 3.2.3 shows a plot of the *ADV*s for the sixty-six pairs of months. The 11AM-3PM TOD period ($t$ = 2) was selected because passenger volumes were highest in this period, which tends to make it most likely to reflect important spatial patterns. The sixty-six *ADV*s are provided in table form in Appendix D.

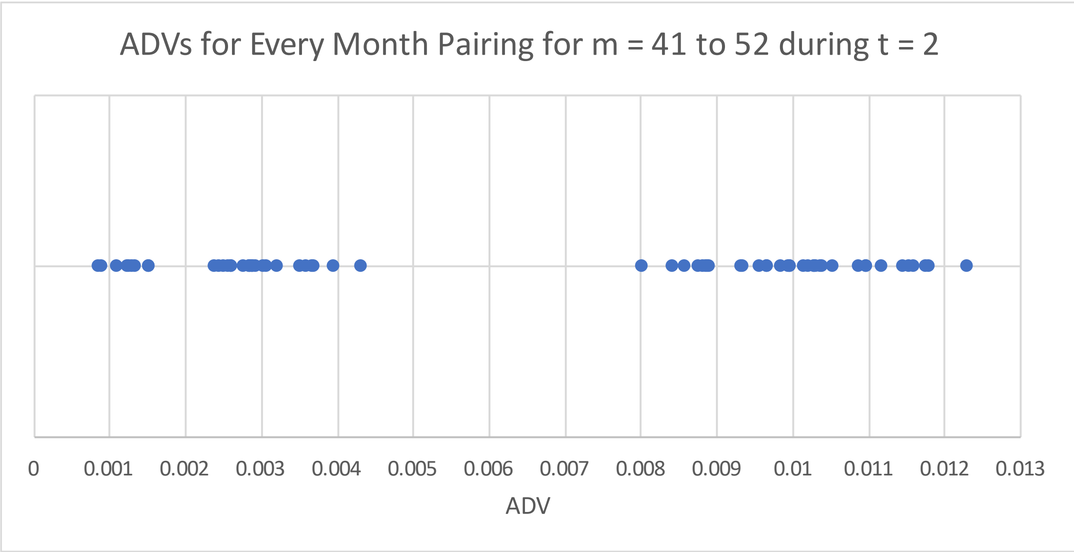


*Figure 3.2.3:* ADV*s for matrices in every pair of months for* m *= 41, 42, …, 52 during the 11AM-3PM TOD period (*t *= 2)*

In Figure 3.2.3, there is a large gap from approximately *ADV* = 0.0045 to *ADV* = 0.0080 that distinguishes two sets of data points. When the data were organized from smallest *ADV* to largest *ADV*, it was noted that small *ADV*s were typically the result of comparisons between matrices in two academic year months or two summer months (with the exception of matrices in August, which typically produced a larger *ADV* when compared to a matrix in any other month). The *ADV*s between autumn and spring semester months were not large or distinct enough to warrant two separate groups. The large *ADV*s were typically the result of comparisons between a matrix in an academic year month and a matrix in May, June, or July or any comparison with a matrix in August. These observations led to the monthly groupings $G_M$ shown in Table 3.2.1, where $G_M = 1$ groups May, June, and July together to represent the summer without August (referred to as the “summer term”); $G_M = 2$ contains only August because all comparisons with August yielded relatively large *ADV*s; and $G_M = 3$ groups September, October, November, December, January, February, March, and April to represent the academic year.

*Table 3.2.1: Groups of months established using* m *= 41 to 52 during TOD period 11AM-3PM* (t *= 2)*

| $G_M$ | Month(s) |
|---|---|
| 1 | MAY, JUN, JUL |
| 2 | AUG |
| 3 | SEP, OCT, NOV, DEC, JAN, FEB, MAR, APR |

3.3. Groups of Months Comparisons

The monthly groupings $G_M$ in Table 3.2.1 were used to specify month(s)-year(s) groupings $G_Y$ over the years. The $G_Y$ specifications are shown in Table 3.3.2. For example, $G_Y = 1$ is the group of months $m = 41$, 42, and 43 (which maps into $G_M = 1$ when referring to Tables 2.2.7 and 3.2.1) in 2021. In Table 3.3.2, a month(s)-year(s) combination is identified by the value(s) of $m$ it contains; the "$G_M$" and "Year(s)" columns are provided in Table 3.3.2 for convenience. $G_Y$s separate the "summer term" months ($G_M = 1$), months of August ($G_M = 2$), and academic year months ($G_M = 3$) by year and will be used to help determine if there are patterns in the OD matrices over the $G_M$s throughout the years.

*Table 3.3.2: Groups of months* $G_M$ *applied over years 2018 through 2022*

| $G_Y$ | $M$ | $G_M$ (see Table 3.2.1) | Year(s) |
|---|---|---|---|
| 1 | 41, 42, 43 | 1 | 2021 |
| 2 | 44 | 2 | 2021 |
| 3 | 45, 46, 47, 48, 49, 50, 51, 52 | 3 | 2021-2022 |
| 4 | 29, 30, 31 | 1 | 2020 |
| 5 | 32 | 2 | 2020 |
| 6 | 33, 34, 35, 36, 37, 38, 39, 40 | 3 | 2020-2021 |
| 7 | 17, 18, 19 | 1 | 2019 |
| 8 | 20 | 2 | 2019 |
| 9 | 21, 22, 23, 24, 25, 26, 27, 28 | 3 | 2019-2020 |
| 10 | 5, 6, 7 | 1 | 2018 |
| 11 | 8 | 2 | 2018 |
| 12 | 9, 10, 11, 12, 13, 14, 15, 16 | 3 | 2018-2019 |

To compare groups of months $G_Y$, a probability matrix that reflects the probability matrices of all of the individual months in the group is determined. An average probability matrix (***APM***) is calculated (Equation 3.3.7) for each group $G_Y$ for a TOD period. The ***APM*** is determined as the average of the probability matrices for a TOD period for all of the months in the group $G_Y$ (Table 3.3.2), where $n$ is the number of months in the group:

$$\boldsymbol{APM_G} = \frac{\sum_{\forall t,m \in G} \boldsymbol{P_{t,m}}}{n},$$

$$m = 41, 42, 43\ for\ t = 1\ with\ n = 3; \dots; m = 9, 10, \dots, 16\ for\ t = 4\ with\ n = 8$$

(3.3.7)

An alternative method of calculating an average probability matrix would be adding the volume OD matrices of all of the months in a group and calculating a probability matrix from the single total OD matrix. Equation 3.3.7 produces a matrix from the monthly probability matrices within a group that is not weighted by the magnitude of the passenger volumes in the months. Using the average of the probability matrix of each month in a group is advantageous because higher-volume months do not have a greater influence on the $\boldsymbol{APM}$. For example, if passenger volumes significantly decrease from April to May, April's spatial pattern would dominate May's spatial pattern if they were grouped together and weighted by volume. In reality, there may be significant spatial changes from April to May that should be equally represented in the group's $\boldsymbol{APM}$. The analysis in this thesis focuses on spatial patterns rather than total volumes, so all of the months in the group should be equally reflected.

Similar to the process of comparing zonal OD matrices for one single month to another, two groups of months are compared by taking the absolute value of the difference between their respective $\boldsymbol{APM}$s, cell by cell, and averaging the cells to calculate the average difference value (*ADV*). Equations 2.3.3 and 2.3.4 in Section 2.3 show the calculations for absolute difference matrices $\boldsymbol{D}$s and *ADV*s, respectively, for comparisons between matrices in single months. The same equations are adapted for matrices in groups of months:

$$\boldsymbol{D_{G_Y;G_{Y'}}} = ABS(\boldsymbol{APM_{G_Y}} - \boldsymbol{APM_{G_{Y'}}}),$$

$$G_Y = 1\ and\ G_Y' = 2\ for\ t = 1; \dots; G_Y = 11\ and\ G_Y' = 12\ for\ t = 4$$

(3.3.8)

$$ADV_{G_Y;G_Y'} = \frac{\sum_{\forall(i,j)} D_{G_Y;G_Y'}(i,j)}{c},$$

$$G_Y = 1 \text{ and } G_Y' = 2 \text{ for } t = 1; \ldots; G_Y = 11 \text{ and } G_Y' = 12 \text{ for } t = 4 \tag{3.3.9}$$

Appendix E contains the data for the comparisons between $G_Y$ pairs. Figures 3.3.4 and 3.3.5 show these comparisons plotted according to whether the comparison is between $G_Y$s belonging to the "same $G_M$" or to "different $G_M$" for all four TOD periods. Figure 3.3.4 shows empirical cumulative distribution functions (ECDFs), while Figure 3.3.5 shows data points as individual observations. As an example, the comparison between $G_Y' = 2$ and $G_Y = 8$ would be between the same $G_M$: $G_M = 2$, which represents the monthly group containing only the month of August (Table 3.2.1). The *ADV* for this comparison is part of the data set plotted in blue in Figures 3.3.4 and 3.3.5. The comparison between $G_Y' = 2$ and $G_Y = 9$ would be between different $G_M$s: $G_Y = 2$ belongs to $G_M = 2$, which represents the monthly group containing only the month of August (Table 3.2.1), while $G_Y = 9$ belongs to $G_M = 3$, which represents the monthly group containing the months of September, October, November, December, January, February, March, and April (Table 3.2.1). The *ADV* for this comparison is part of the data set plotted in orange in Figures 3.3.4 and 3.3.5. Table 3.3.3 contains the mean, median, and standard deviation values for the data sets "Between Same $G_M$" and "Between Different $G_M$" by TOD period.

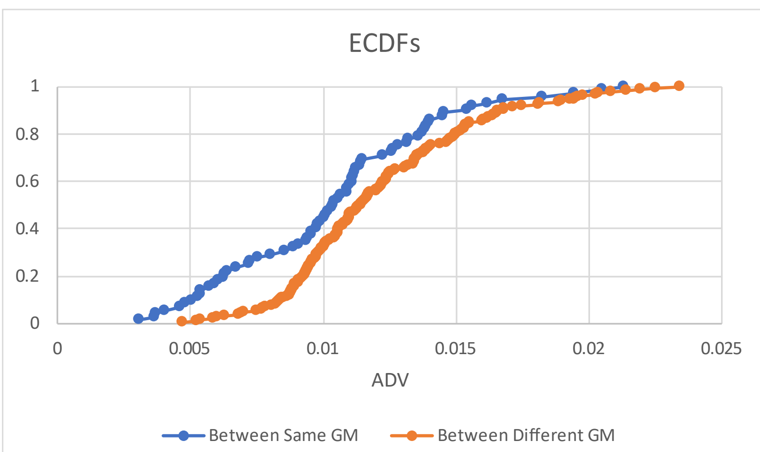


*Figure 3.3.4: ECDFs for* ADVs *for every* $G_Y$ *with every other* $G_Y$ *organized according to same/different* $G_M$

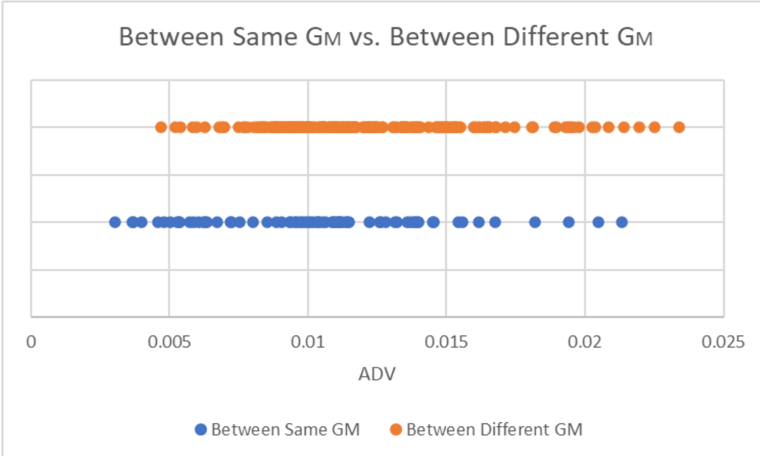


*Figure 3.3.5: Plot of* ADVs *for every* $G_Y$ *with every other* $G_Y$ *organized according to* $G_M$

*Table 3.3.3: Mean, median, and standard deviation of "Between Same* $G_M$*" and "Between Different* $G_M$*" comparisons by TOD period* (t)

| TOD Period | 7-11AM ($t$ = 1) | | 11AM-3PM ($t$ = 2) | | 3-6PM ($t$ = 3) | | 6-9PM ($t$ = 4) | |
|---|---|---|---|---|---|---|---|---|
| | Between Same $G_M$ | Between Different $G_M$ | Between Same $G_M$ | Between Different $G_M$ | Between Same $G_M$ | Between Different $G_M$ | Between Same $G_M$ | Between Different $G_M$ |
| Mean | 0.01074 | 0.01228 | 0.00924 | 0.01094 | 0.00980 | 0.01122 | 0.01181 | 0.01407 |
| Median | 0.01014 | 0.01113 | 0.00990 | 0.01043 | 0.01019 | 0.01118 | 0.01129 | 0.01367 |
| St. Dev. | 0.00509 | 0.00430 | 0.00335 | 0.00247 | 0.00345 | 0.00270 | 0.00391 | 0.00378 |

Figure 3.3.4 shows that the ECDF for comparisons between the same $G_M$ lies to the left of the ECDF for comparisons between different $G_M$s. This indicates consistently lower *ADV*s between $G_Y$ matrices that belong to the same $G_M$ than between those that belong to different $G_M$s. That is, the matrices for groups of months determined to be similar ("homogenous") in flow patterns in the 2021 to 2022 year are more similar to each other over the years than to matrices belonging to other groups of homogenous months. For example, this would reflect that, in general, the summer term 2019 spatial flow pattern would tend to be more similar to the summer term 2020 flow pattern than to the academic year 2019-2020 flow pattern. Similarly, the academic year 2018-2019 pattern would tend to be more similar to the academic year 2019-2020 pattern than to the summer term 2019 pattern.

It was expected that comparisons between $G_Y$s belonging to the same $G_M$ would produce smaller $ADV$s than comparisons between $G_Y$s belonging to different $G_M$s because of the similarities in spatial flow patterns for months within the same group discussed in Section 3.2. The monthly groups are intended to represent homogenous periods. Figure 3.3.4 reflects this expectation. Table 3.3.3 summarizes the plots in Figures 3.3.4 and 3.3.5. The mean and median values of $ADV$s between $G_Y$s belonging to different $G_M$s are larger than the mean and median values between $G_Y$s belonging to the same $G_M$ for each TOD period ($t$ = 1, 2, 3, and 4). This is consistent with the interpretation of the ECDFs in Figure 3.3.4 that comparisons between $G_Y$s belonging to the same $G_M$ produce smaller $ADV$s than comparisons between $G_Y$s belonging to different $G_M$s.

However, Figure 3.3.5 shows that there is a lot of overlap in $ADV$s for comparisons between $G_Y$ that belong to the same $G_M$ and $ADV$s for comparisons between $G_Y$ that belong to different $G_M$. For example, $G_Y' = 1$ and $G_Y = 4$ belong to the same $G_M = 1$. Comparison of their average probability matrices produces $ADV = 0.019417156$ for the 7-11AM TOD period ($t = 1$). This is a very large value relative to the data set, which is not necessarily expected for comparisons between $G_Y$ that belong to the same $G_M$. Another example is $G_Y' = 7$ and $G_Y = 8$, which belong to $G_M = 1$ and $G_M = 2$, respectively. Comparison of their average probability matrices produces $ADV = 0.004707329$ for the 7-11AM TOD period ($t = 1$). This is a very small value relative to the data set, which is not necessarily expected for comparisons between $G_Y$ that belong to different $G_M$s. This could indicate that there are some notable changes in spatial flow patterns within groups of months $G_M$ over the years 2018 through 2022. For example, one August flow pattern may be more similar to the academic year that follows it than to an August flow pattern from a different year.

To further investigate when spatial shifts are occurring over time, the "Between Same $G_M$" ECDF is decomposed into three ECDFs representing results from comparisons between $G_Y$s belonging to the same monthly group $G_M$. That is, one ECDF is determined for comparisons between $G_Y$s belonging to $G_M$ = 1 (summer term), a second for $G_M$ = 2 (AUG), and a third for $G_M$ = 3 (academic year). These ECDFs are shown in Figure 3.3.6. The ECDF for comparisons between $G_Y$s belonging to different $G_M$s from Figure 3.3.4 is also plotted in Figure 3.3.6 for comparison purposes.

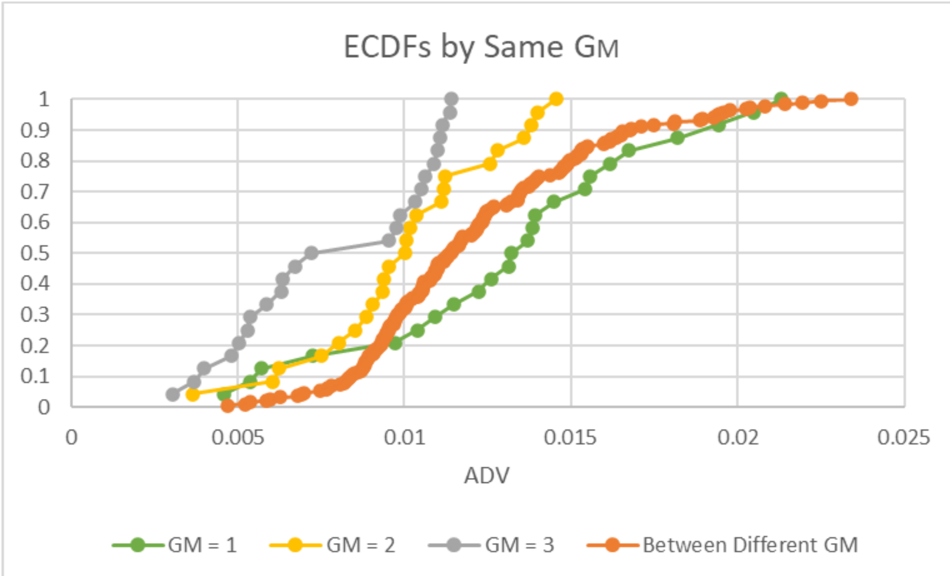


*Figure 3.3.6: ECDFs for* ADVs *for every* $G_Y$ *with every other* $G_Y$ *organized according to* $G_M$

Figure 3.3.6 distinguishes between different subcomponents within the "between same $G_M$" comparisons data set. The $G_M$ = 3 (academic years) ECDF is farthest left, the $G_M$ = 1 (summer terms) is farthest right, and the $G_M$ = 2 (AUG) falls between them. That is, comparisons between academic years are smallest and comparisons between summer terms are largest. Summer term comparisons are, generally, even larger than "different $G_M$" comparisons. One explanation for the large differences between summer term $G_Y$s could be changes in the month of May from year to year. May includes the end of the spring semester, a period of time when there are no classes in session, and the start of summer term classes. This could lead to greater differences between summer term $G_Y$s.

Appendix F contains a table for each ECDF in Figure 3.3.6 with data points organized from smallest to largest *ADV*. It is noted that comparisons between academic years ($G_M$ = 3) exhibit a bimodal distribution. This is indicated by the break in the ECDF in Figure 3.3.6 from *ADV* = 0.007201 to *ADV* = 0.009548. This break is also seen in Appendix F Table F.3. *ADV*s for academic year comparisons that are less than 0.0075 are a result of comparisons among $G_Y$ = 3, 9, and 12. *ADV*s for academic year comparisons that are greater than 0.0075 are a result of comparisons with $G_Y = 6$, which is the academic year 2020-2021. It appears that changes in flow patterns resulting from the online/hybrid nature of classes, fewer students living on campus, and the lack of nonessential workers coming to and from campus were indicated by the *ADV* metric within the $G_Y$ comparisons.

Appendix F Table F.1 shows *ADV*s for comparisons between matrices for pairs of $G_Y$s belonging to $G_M = 1$. *ADV*s in the left part of the distribution (smaller than *ADV* = 0.0075) compare two pre-lockdown $G_Y$s. The four smallest *ADV*s for comparisons between $G_Y$s belonging to $G_M = 1$ are for comparisons between $G_Y = 7$ (summer term of 2019) and $G_Y = 10$ (summer term of 2018) for the four TOD periods. Appendix F Table F.2 shows *ADV*s for comparisons between matrices for pairs of $G_Y$s belonging to $G_M = 2$. *ADV*s smaller than 0.0075 also compare two pre-lockdown $G_Y$s. The three smallest *ADV*s within $G_M = 2$ are for comparisons between $G_Y = 8$ (AUG of 2019) and $G_Y = 11$ (AUG of 2018) for all but the 6-9PM TOD period. Appendix F Table F.3 shows *ADV*s for comparisons between matrices for pairs of $G_Y$s belonging to $G_M = 3$. *ADV*s smaller than 0.0075 also compare two pre-lockdown $G_Y$s. The three smallest *ADV*s within $G_M = 3$ are for comparisons between $G_Y = 9$ (academic year 2019-2020) and $G_Y = 12$ (academic year 2018-2019) for all but the 6-9PM TOD period. Because pre-lockdown comparisons yield the smallest *ADV*s within all three $G_M$s, spatial patterns appear to be most stable before the onset of the COVID-19 pandemic, with changes from these patterns observed through the end of 2022.

The next smallest *ADV*s for $G_M = 1$, $G_M = 2$, and $G_M = 3$ occur for comparisons between post-lockdown matrices and pre-lockdown matrices. For example, the six next smallest *ADV*s within $G_M = 1$ are for comparisons between $G_Y = 1$ (summer term of 2021) and $G_Y = 7$ or 10 (summer term of 2019 or 2018, respectively) for all but the 6-9PM TOD period. Within $G_M = 2$, all but one of the six next smallest *ADV*s are between $G_Y = 2$ (AUG of 2021) and $G_Y = 8$ or 11 (AUG of 2019 or 2018, respectively). Within $G_M = 3$, all but one of the nine next smallest *ADV*s are between $G_Y = 3$ (academic year 2021-2022) and $G_Y$ = 9 or 12 (academic year 2019-2020 or 2018-2019, respectively). All of these “next smallest” *ADV*s are the result of comparisons between more recent years (2021 and 2022) and pre-lockdown years (2018 and 2019). These patterns, especially for the academic year, indicate that matrices from pre-lockdown $G_Y$s and post-lockdown $G_Y$s belonging to the same $G_M$ have more spatial similarity than matrices from pre-lockdown/post-lockdown $G_Y$s and during-lockdown $G_Y$s belonging to the same $G_M$. Figure 3.3.7 shows the *ADV*s for $G_Y$ comparisons belonging to the same $G_M = 3$ plotted as individual observations organized by combination of "pre"-, "during"-, and "post"-lockdown $G_Y$s. The same type of plot for $G_M = 1$ and $G_M = 2$ are located in Appendix G. The figure highlights how pre- and post-lockdown matrices (represented by yellow points) are more different from each other than pre- and pre-lockdown matrices (blue points), but post-lockdown matrices are more similar to pre-lockdown matrices (yellow points) than they are to during-lockdown matrices (gray points). Moreover, the pre-lockdown matrices are more similar to post-lockdown matrices (yellow points) than they are to during-lockdown matrices (orange points). This pattern in the comparisons could indicate a gradual return to pre-lockdown spatial flow patterns, or it could reveal lasting structural changes in these patterns.

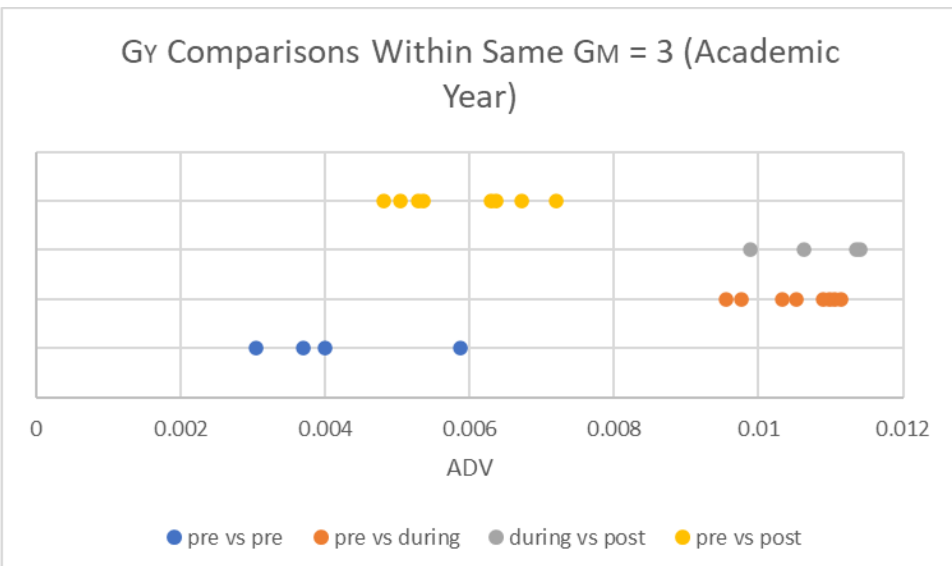


*Figure 3.3.7: Plot of* ADV*s for comparisons between* $G_Y$*s belonging to the same* $G_M$ *= 3 (academic year)*

The results of this analysis demonstrate the ability of the metric to retroactively identify patterns in spatial flow patterns that otherwise may not have been evident. As discussed in Section 4.2, the results also motivate further investigation into what OD pairs are contributing to small versus large *ADV*s to develop a better understanding of spatial shifts occurring over time.

# Chapter 4: Summary and Conclusion

## 4.1. Summary and Conclusion

In this thesis, an average difference value (ADV) metric was developed to monitor spatial patterns in zonal OD matrices and groups of matrices to identify homogenous patterns, recurring differences, and singular changes in the matrices. When applied to historical matrices for bus travel on The Ohio State University campus, the metric was able to detect expected changes and similarities in spatial patterns over time. These expected changes included changes between academic year matrices and summer matrices that recurred yearly on OSU's campus and singular changes due to COVID-19 policies implemented by the university. When comparing matrices in consecutive months, the metric showed large differences between the last summer month and the first academic year month and between the last academic year month and the first summer month. There were relatively small differences for comparisons between matrices in consecutive academic year months and matrices in consecutive summer months. The metric showed a large difference in spatial patterns between matrices from 03/2020 and 04/2020 in connection to the implementation of OSU's COVID-19 policies. These results validated the *ADV* metric.

The metric was then used to identify other spatial patterns and changes specific to the OSU campus over time. To do so, several empirical analyses were conducted. Consecutive months comparisons between matrices in the 6-9PM time-of-day (TOD) period showed greater differences than those in the other three TOD periods but followed a similar pattern. This means there were larger changes in spatial patterns from month to month during the 6-9PM TOD period than during other TOD periods.

Homogenous monthly groups were developed by using the metric to compare all the pairs of monthly matrices within a one-year period to identify and group months with similar zonal flow patterns. These monthly groups were applied across the years of historical data to detect similarities and changes in passenger spatial patterns over time. Analysis of the monthly groups showed that some stability in spatial patterns was maintained over the years. However, comparisons involving matrices for groups of months impacted by COVID-19 policies, in which most nonessential travel on the OSU campus was “locked down,” revealed large changes in spatial patterns. Comparisons between two pre-lockdown matrices generally showed the smallest differences. Comparisons between pre- and post-lockdown matrices generally showed smaller differences than comparisons between pre- and during-lockdown matrices and comparisons between during- and post-lockdown matrices. Similarity between pre- and post-lockdown matrices could indicate a gradual return to pre-lockdown spatial flow patterns, or it could reflect a lasting structural change in spatial flow patterns on the OSU campus post-lockdown.

## 4.2. Future Work

The metric developed in this thesis and the empirical values determined could be used to assess the impacts of transit service changes, such as changes to CABS routes made during autumn 2022 on the OSU campus. *ADV*s could be determined by comparing matrices obtained before the changes to matrices obtained after the changes for the same $G_M$ and TOD period. The resulting values could then be compared to distributions of *ADV*s obtained in the empirical analysis of Section 3.3 to determine if the values obtained from the “before” and “after” comparisons would be considered small or large.

Future work could also include analyzing the difference matrices $\boldsymbol{D}$ (see Section 2.3) that produce large *ADV*s to develop a quantifiable process that determines whether large *ADV*s result from relatively uniform differences across cells or from a few “standout” cells in the difference matrix. Standout cells could indicate geographic zones pairs between which passenger flows are changing greatly from one matrix to another.

The time-of-day (TOD) periods used for analysis in this thesis have been used by CTL for several years for the purpose of estimating time-varying OD matrices that are provided to TTM. Repeating the analysis conducted in Chapter 3 with more refined TOD periods would indicate whether the interesting similarities and changes detected through application of the *ADV* metric seen in this thesis are sensitive to minor or major modification in these specifications. Similarly, it would be interesting to repeat the analysis with modification or refinements of zone specifications. The geographical zones used in this thesis were developed in collaboration with CTL and TTM prior to this research project and are now used in determining the monthly zonal OD matrices that are provided to TTM. Nevertheless, finer resolution zones could be considered for research into whether the homogenous patterns, recurring differences, and singular changes identified on the OSU campus would be the same when considering modified or smaller geographic areas.

References


Chen, A. (2020). *Bus Transit Passenger Origin-destination Flow Estimation: Capturing Terminal Carry-over Movements Using the Iterative Proportional Fitting Method* (M.S. thesis). The Ohio State University.

Deming, W. E., & Stephan, F. F. (1940, December). *On a Least Squares Adjustment of a Sampled Frequency Table When the Expected Marginal Totals are Known*. Project Euclid. Retrieved from https://projecteuclid.org/journals/annals-of-mathematical-statistics/volume-11/issue-4/On-a-Least-Squares-Adjustment-of-a-Sampled-Frequency-Table/10.1214/aoms/1177731829.full.

Horowitz, A., Creasey, T., Pendyala, R., & Chen, M. (2014). Analytical Travel Forecasting Approaches for Project-Level Planning and Design. *The National Academies Press*. https://doi.org/10.17226/22366.

Ji, Y., Mishalani, R. G., & McCord, M. R. (2014). Estimating Transit Route OD Flow Matrices from APC Data on Multiple Bus Trips Using the IPF Method with an Iteratively Improved Base: Method and Empirical Evaluation. *Journal of Transportation Engineering*, *140*(5). https://doi.org/10.1061/(asce)te.1943-5436.0000647.

Ji, Y., Mishalani, R. G., & McCord, M. R. (2015). Transit passenger origin–destination flow estimation: Efficiently combining onboard survey and large automatic passenger count datasets. *Transportation Research Part C: Emerging Technologies*, *58*, 178–192. https://doi.org/10.1016/j.trc.2015.04.021.

Ji, Y., Mishalani, R. G., McCord, M. R., & Goel, P. K. (2011). Identifying Homogeneous Periods in Bus Route Origin-Destination Passenger Flow Patterns from Automatic Passenger Counter Data. *Transportation Research Record*, *2216*(1), 42–50. https://doi.org/10.3141/2216-05.

Kruithof, J. (n.d.). *Telephone traffic computation ("Telefoonverkeersrekening")*. Retrieved from https://wwwhome.ewi.utwente.nl/~ptdeboer/misc/kruithof-1937-translation.html.

McCord, M. R., Mishalani, R. G., Goel, P. K., & Strohl, B. (2010). Empirical Comparative Assessment of the IPF Procedure for Determining Bus Route Passenger OD Flows. *Transportation Research Record*, (2145), 59–65.

Meyer, M., & Miller, E. J. (2001). *Urban Transportation Planning: A Decision-Oriented Approach* (2nd ed.). McGraw-Hill.

Reinhold, H. (2013). *Combining Transit Route Origin-Destination Passenger Flow Matrices into Integrated Area or Corridor Matrices: Evaluating Flow Patterns on the OSU Campus and along a Columbus Corridor* (M.S. thesis). The Ohio State University.

Appendix A: CABS Routes Maps and Lists of Stops

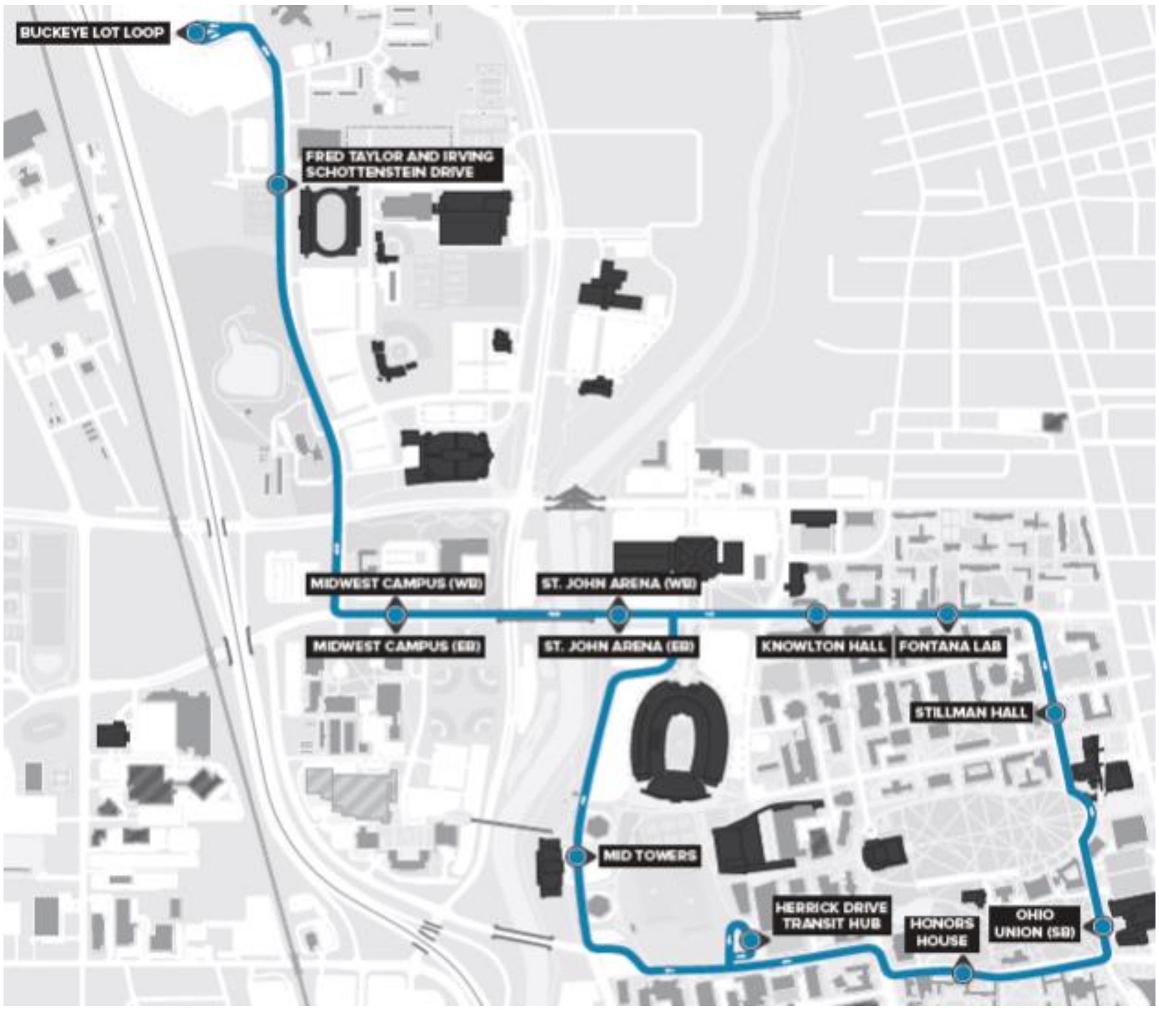


*Figure A.1: Map of Campus Loop North bus route (obtained from monthly reports to the Transportation and Traffic Management office)*

*Table A.1: List of Campus Loop North bus route stops*

| Stop No. | Name |
|---|---|
| 1 | Fred Taylor and Irving Schottenstein Drive |
| 2 | Buckeye Lot Loop |
| 3 | Midwest Campus (EB) |
| 4 | St. John Arena (EB) |
| 5 | Knowlton Hall |
| 6 | Fontana Lab |
| 7 | Stillman Hall |
| 8 | Ohio Union (SB) |
| 9 | Honors House |
| 10 | Herrick Transit Hub |
| 11 | Mid Towers |
| 12 | St. John Arena (WB) |
| 13 | Midwest Campus (WB) |

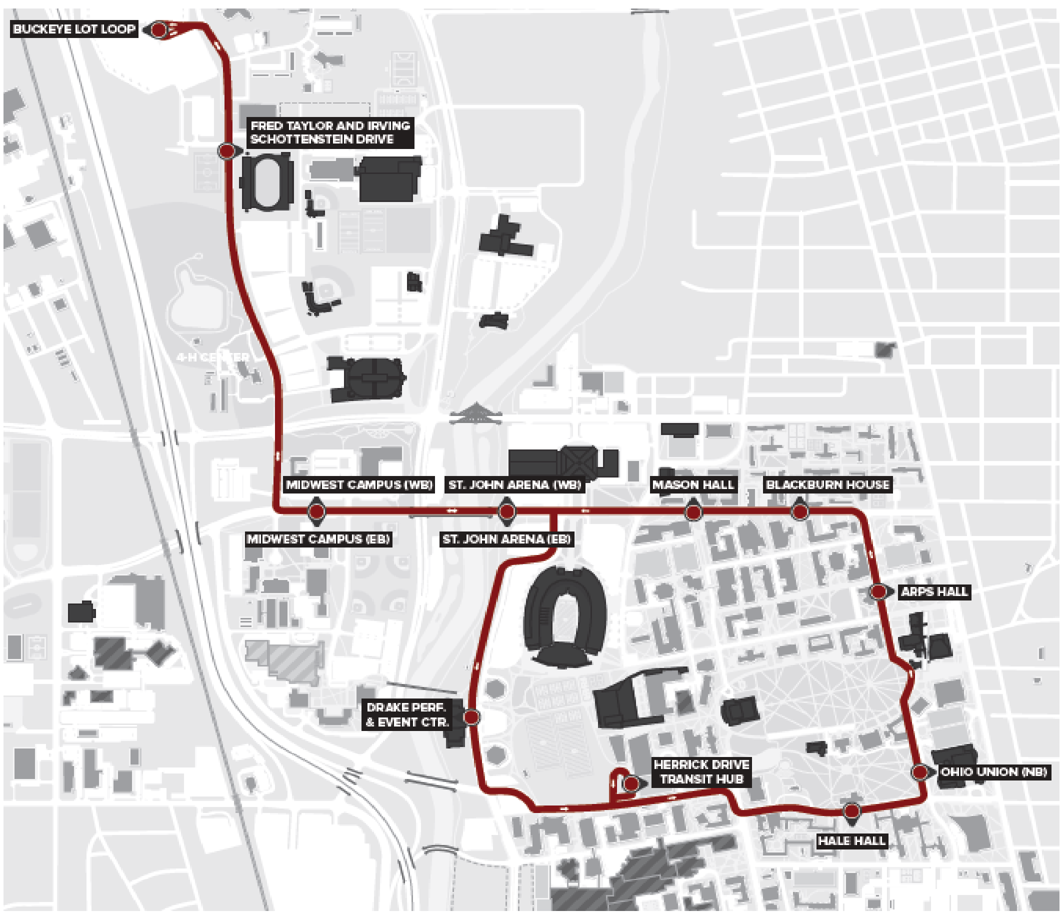


*Figure A.2: Map of Campus Loop South bus route (obtained from monthly reports to the Transportation and Traffic Management office)*

*Table A.2: List of Campus Loop South bus route stops*

| Stop No. | Name |
|---|---|
| 1 | Fred Taylor and Irving Schottenstein Drive |
| 2 | Buckeye Lot Loop |
| 3 | Midwest Campus (EB) |
| 4 | St. John Arena (EB) |
| 5 | Drake Center |
| 6 | Herrick Transit Hub |
| 7 | Hale Hall |
| 8 | Ohio Union (NB) |
| 9 | Arps Hall |
| 10 | Blackburn House |
| 11 | Mason Hall |
| 12 | St. John Arena (WB) |
| 13 | Midwest Campus (WB) |

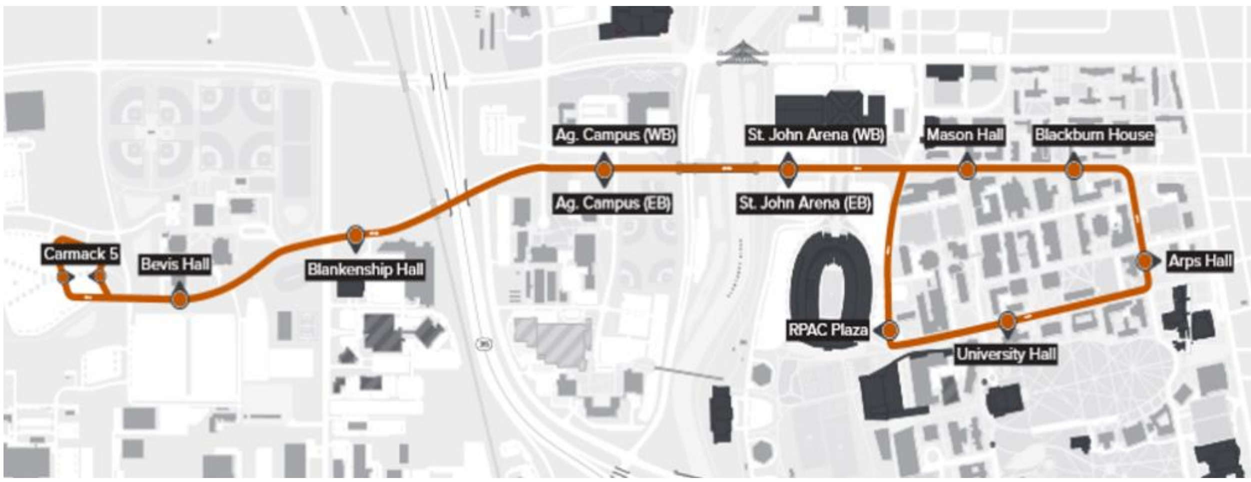


*Figure A.3: Map of North Express bus route (obtained from monthly reports to the Transportation and Traffic Management office)*

*Table A.3: List of North Express bus route stops*

| Stop No. | Name |
|---|---|
| 1<br>Boarding<br>Terminal | Bevis Hall<br>Carmack 5A<br>Carmack 5B |
| 2 | Blankenship Hall |
| 3 | AG Campus (EB) |
| 4 | St. John (EB) |
| 5 | RPAC Plaza |
| 6 | University Hall |
| 7 | Arps Hall |
| 8 | Blackburn House |
| 9 | Mason Hall |
| 10 | St. John (WB) |
| 11 | AG Campus (WB) |

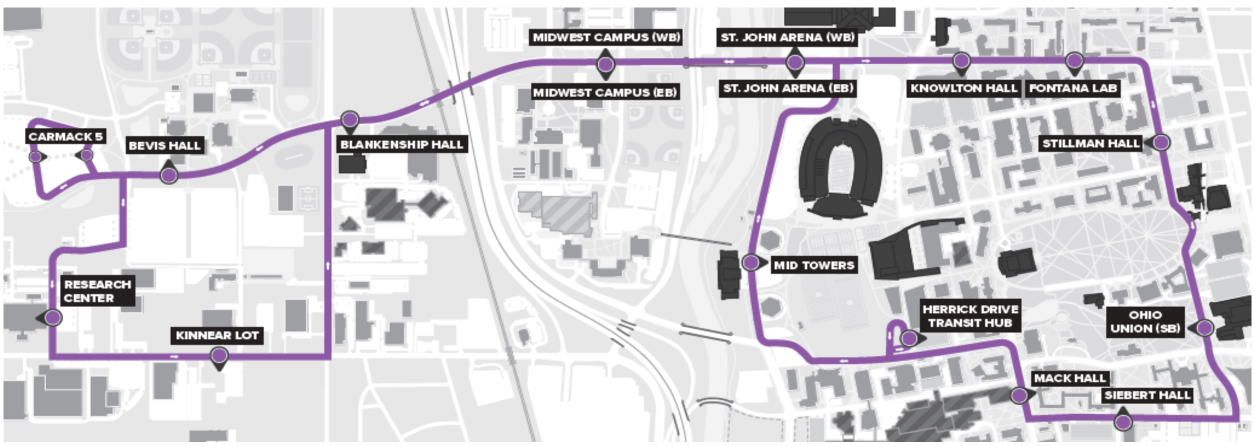


*Figure A.4: Map of West Campus bus route (obtained from monthly reports to the Transportation and Traffic Management office)*

*Table A.4: List of West Campus bus route stops*

| Stop No. | Name |
|---|---|
| 1 | Bevis Hall |
| 2 | Carmack 5A |
| 3 | Carmack 5B |
| 4 | Research Center |
| 5 | Kinnear Road Lot |
| 6 | Blankenship Hall |
| 7 | Midwest Campus (EB) |
| 8 | St. John Arena (EB) |
| 9 | Knowlton Hall |
| 10 | Fontana Lab |
| 11 | Stillman Hall |
| 12 | Ohio Union (SB) |
| 13 | Siebert Hall |
| 14 | Mack Hall |
| 15 | Herrick Transit Hub |
| 16 | Mid Towers |
| 17 | St. John Arena (WB) |
| 18 | Midwest Campus (WB) |

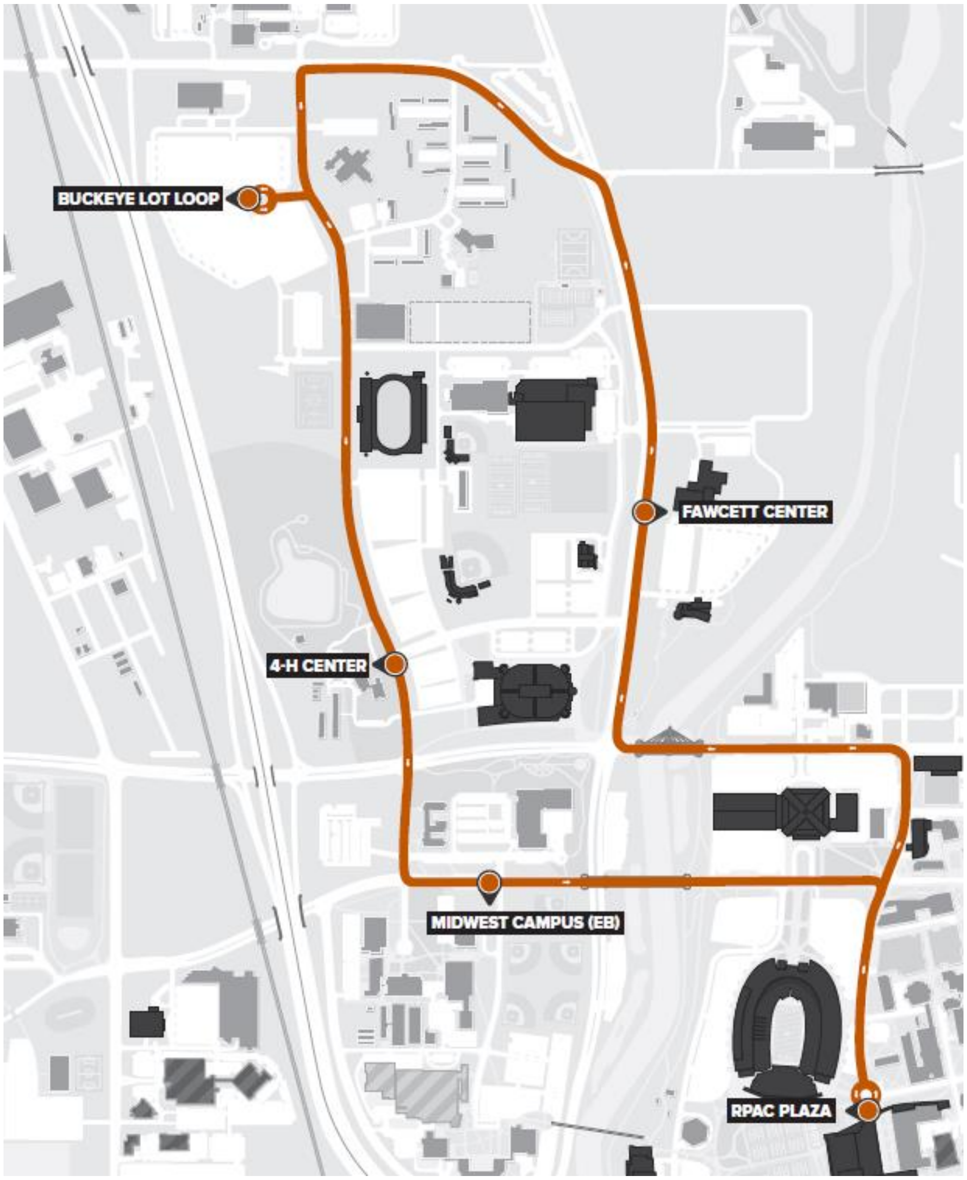

*Figure A.5: Map of Buckeye Loop bus route (obtained from Campus Transit Laboratory research engineer)*

*Table A.5: List of Buckeye Loop bus route stops*

| Stop No. | Name |
|---|---|
| 1 | Buckeye Lot Loop |
| 2 | 4-H Center |
| 3 | AG Campus (EB) |
| 4 | RPAC Plaza |
| 5 | Fawcett Center |

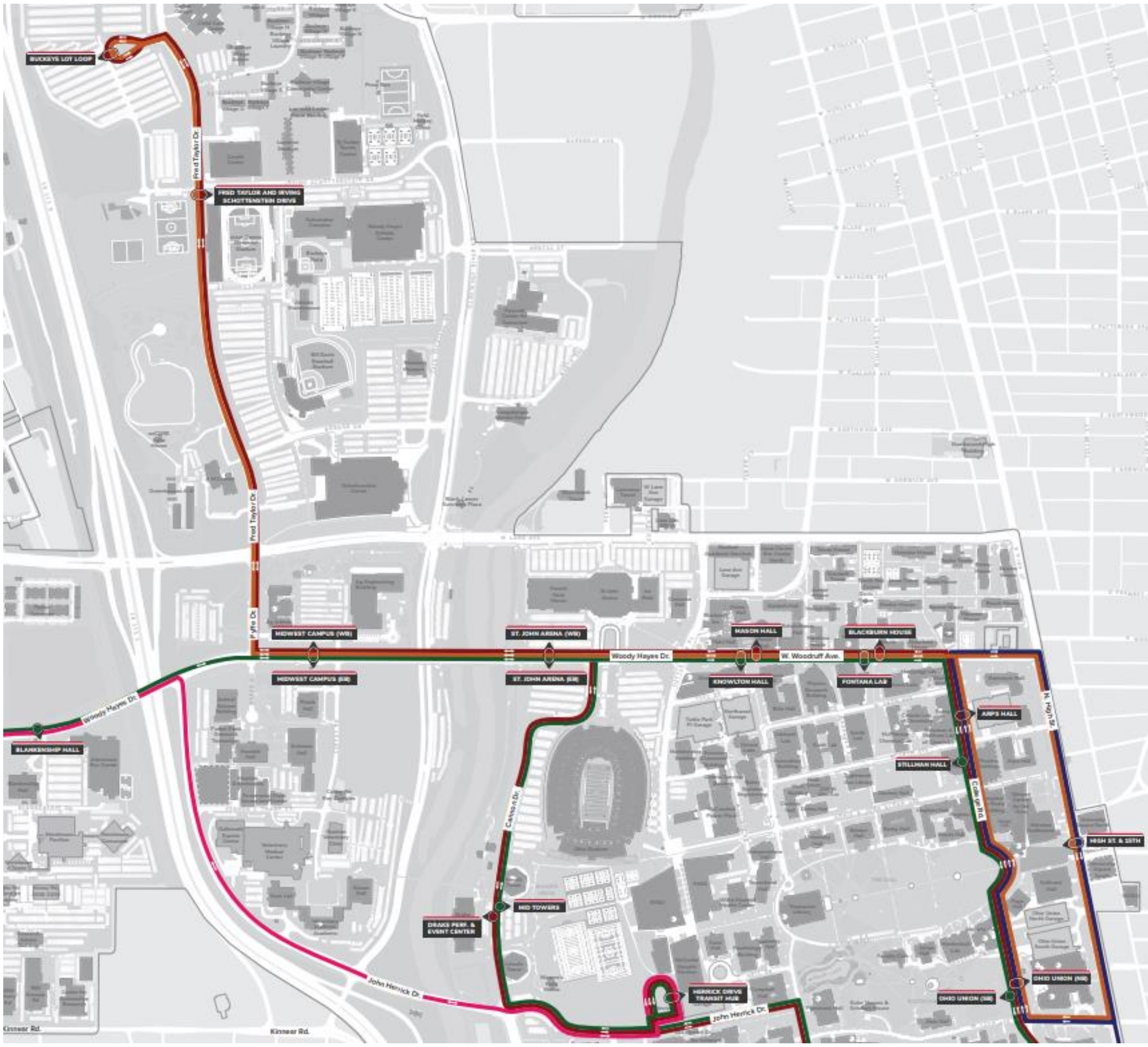


*Figure A.6: Map of Buckeye Express bus route (orange) (obtained from monthly reports to the Transportation and Traffic Management office)*

*Table A.6: List of Buckeye Express bus route stops*

| Stop No. | Name |
|---|---|
| 1 | Fred Taylor & Schottenstein Drive |
| 2 | Buckeye Lot Loop |
| 3 | AG Campus (EB) |
| 4 | St John Arena (EB) |
| 5 | Knowlton Hall |
| 6 | Fontana Lab |
| 7 | High and 15$^{th}$ |
| 8 | Ohio Union (NB) |
| 9 | Arps Garage |
| 10 | Blackburn |
| 11 | Mason |
| 12 | St John Arena (WB) |
| 13 | AG Campus (WB) |

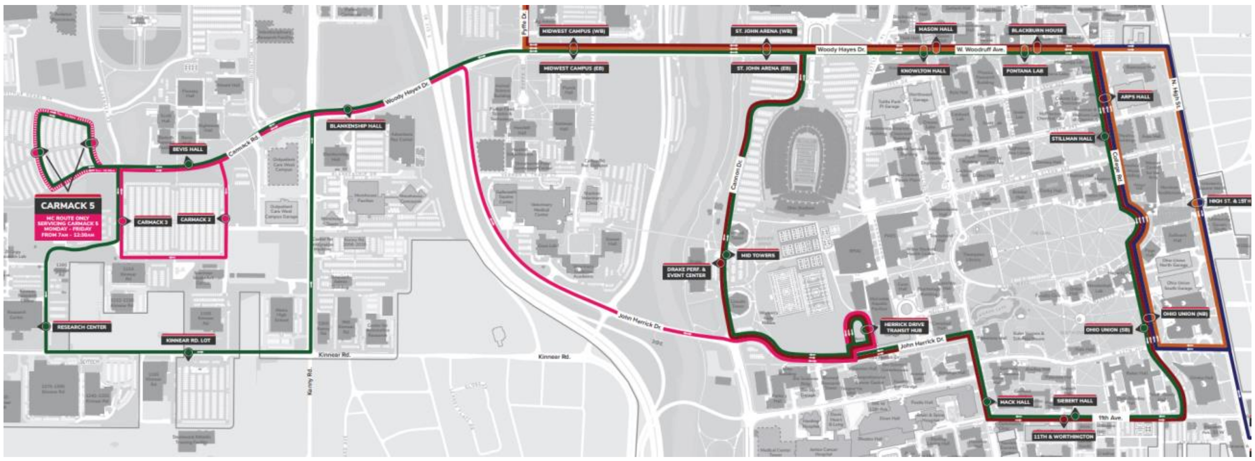


*Figure A.7: Map of Campus Connector bus route (green) (obtained from monthly reports to the Transportation and Traffic Management office)*

*Table A.7: List of Campus Connector bus route stops*

| Stop No. | Name |
|---|---|
| 1 | Bevis Hall |
| 2 | Carmack 5A |
| 3 | Carmack 5B |
| 4 | Research Center |
| 5 | Kinnear Road Lot |
| 6 | Blankenship Hall |
| 7 | AG Campus (EB) |
| 8 | St John Arena (EB) |
| 9 | Knowlton Hall |
| 10 | Fontana Lab |
| 11 | Stillman Hall |
| 12 | Ohio Union (SB) |
| 13 | Siebert Hall |
| 14 | Mack Hall |
| 15 | Herrick Transit Hub |
| 16 | Mid Towers |
| 17 | St John Arena (WB) |
| 18 | AG Campus (WB) |

Appendix B: CABS Routes in Operation by Month

*Table B.1: CABS Routes in operation by month-year combination*

| Month-Year Combination | Routes in Operation |
|---|---|
| January 2018 | CLN, CLS, NE, WC |
| February 2018 | CLN, CLS, NE, WC |
| March 2018 | CLN, CLS, NE, WC |
| April 2018 | CLN, CLS, NE, WC |
| May 2018 | CLN, CLS, NE, WC |
| June 2018 | CLN, CLS, WC |
| July 2018 | CLN, CLS, WC |
| August 2018* | CLN, CLS, WC |
| September 2018 | CLN, CLS, NE, WC |
| October 2018 | CLN, CLS, NE, WC |
| November 2018 | CLN, CLS, NE, WC |
| December 2018 | CLN, CLS, NE, WC |
| January 2019 | CLN, CLS, NE, WC |
| February 2019 | CLN, CLS, NE, WC |
| March 2019 | CLN, CLS, NE, WC |
| April 2019 | CLN, CLS, NE, WC |
| May 2019 | CLN, CLS, WC |
| June 2019 | CLN, CLS, WC |
| July 2019 | CLN, CLS, WC |
| August 2019* | CLN, CLS, WC |
| September 2019 | CLN, CLS, NE, WC |
| October 2019 | CLN, CLS, NE, WC |
| November 2019 | CLN, CLS, NE, WC |
| December 2019 | CLN, CLS, NE, WC |
| January 2020 | CLN, CLS, NE, WC |
| February 2020 | CLN, CLS, NE, WC |
| March 2020 | CLN, CLS, NE, WC |
| April 2020 | CLN, CLS, WC |
| May 2020 | CLN, CLS, WC |
| June 2020 | CLN, CLS, WC |

| | |
|---|---|
| July 2020 | CLN, CLS, WC |
| August 2020* | CLN, CLS, WC |
| September 2020 | BL, CLS, WC |
| October 2020 | BL, CLS, WC |
| November 2020 | BL, CLS, WC |
| December 2020 | CLS, WC |
| January 2021 | BL, CLS, WC |
| February 2021 | BL, CLS, WC |
| March 2021 | BL, CLS, WC |
| April 2021 | BL, CLS, WC |
| May 2021 | CLS, WC |
| June 2021 | CLS, WC |
| July 2021 | CLS, WC |
| August 2021* | CLS, WC |
| September 2021 | CLN, CLS, WC |
| October 2021 | CLN, CLS, WC |
| November 2021 | CLN, CLS, WC |
| December 2021 | CLN, CLS, WC |
| January 2022 | CLN, CLS, WC |
| February 2022 | CLN, CLS, WC |
| March 2022 | CLN, CLS, WC |
| April 2022 | CLN, CLS, WC |
| May 2022 | CLN, CLS, WC |
| June 2022 | CLN, CLS, WC |
| July 2022 | CLN, CLS, WC |
| August 2022* | CLN, CLS, WC |
| September 2022 | BE, CC |
| October 2022 | BE, CC |
| November 2022 | BE, CC, CLS |
| December 2022 | BE, CC, CLS |

* months of August show routes operating during the summer portion of the month

Appendix C: Matrices Using Boarding vs. Alighting Times to Sort Data into TOD Periods

To compare OD matrices produced using passenger boarding times and OD matrices produced using passenger alighting times, a simplified set of zones (shown in Figure C.1) was used to produce zonal OD matrices from the software. For 01/2022, one pair of zonal OD matrices (one using boarding times and another using alighting times) was produced for CLN, CLS, and WC for each TOD period. To investigate the relationship between matrices produced using boarding times and matrices produced using alighting times, zonal OD matrices were determined by route rather than combining all routes into single matrices by TOD period. The correlation coefficient values are shown in Table C.1.

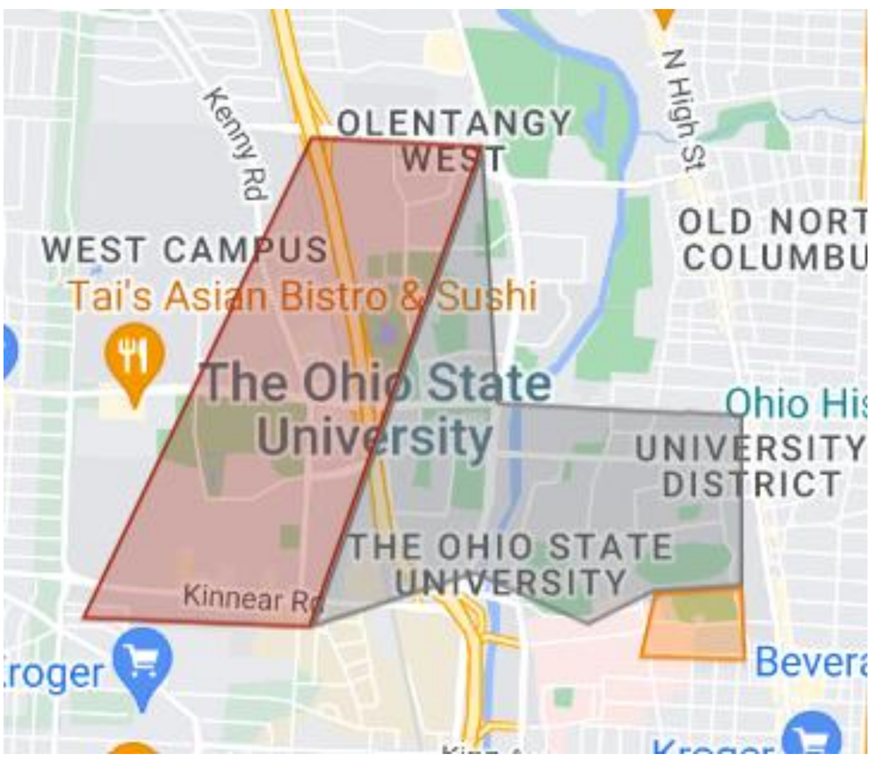


*Figure C.1: Zones used for comparison between matrices produced using boarding times and matrices produced using alighting times*

*Table C.1: Correlation coefficient values between matrices produced using boarding times and matrices produced using alighting times*

| Route | TOD period | Correlation Coefficient |
|---|---|---|
| CLN | 7-11AM | 0.999843245 |
| | 11AM-3PM | 0.996803831 |
| | 3-6PM | 0.998982541 |
| | 6-9PM | 0.999681081 |
| CLS | 7-11AM | 0.999822176 |
| | 11AM-3PM | 0.999383619 |
| | 3-6PM | 0.998271459 |
| | 6-9PM | 0.999624555 |
| WC | 7-11AM | 0.999822176 |
| | 11AM-3PM | 0.999383619 |
| | 3-6PM | 0.998271459 |
| | 6-9PM | 0.999624555 |

Appendix D: *ADV*s for Determination of Homogenous Groups of Months

*Table D.1:* ADVs *for matrices in every pair of months for* m *= 41, 42, …, 52 during the 11AM-3PM TOD period (*t *= 2)*

| MM/YYYY | | MM/YYYY | ADV |
|---|---|---|---|
| 05/2021 | vs. | 06/2021 | 0.004310185 |
| 05/2021 | vs. | 07/2021 | 0.003946883 |
| 05/2021 | vs. | 08/2021 | 0.00997006 |
| 05/2021 | vs. | 09/2021 | 0.00889249 |
| 05/2021 | vs. | 10/2021 | 0.008816204 |
| 05/2021 | vs. | 11/2021 | 0.009310813 |
| 05/2021 | vs. | 12/2021 | 0.0088641 |
| 05/2021 | vs. | 01/2022 | 0.010305133 |
| 05/2021 | vs. | 02/2022 | 0.01052652 |
| 05/2021 | vs. | 03/2022 | 0.009561741 |
| 05/2021 | vs. | 04/2022 | 0.009657416 |
| 06/2021 | vs. | 07/2021 | 0.003512444 |
| 06/2021 | vs. | 08/2021 | 0.011165162 |
| 06/2021 | vs. | 09/2021 | 0.010356755 |
| 06/2021 | vs. | 10/2021 | 0.010284669 |
| 06/2021 | vs. | 11/2021 | 0.010387739 |
| 06/2021 | vs. | 12/2021 | 0.0102925 |
| 06/2021 | vs. | 01/2022 | 0.011743865 |
| 06/2021 | vs. | 02/2022 | 0.012287667 |
| 06/2021 | vs. | 03/2022 | 0.011447733 |
| 06/2021 | vs. | 04/2022 | 0.011592839 |
| 07/2021 | vs. | 08/2021 | 0.010976502 |
| 07/2021 | vs. | 09/2021 | 0.009949222 |
| 07/2021 | vs. | 10/2021 | 0.009955057 |
| 07/2021 | vs. | 11/2021 | 0.010206222 |
| 07/2021 | vs. | 12/2021 | 0.010138449 |
| 07/2021 | vs. | 01/2022 | 0.011536126 |
| 07/2021 | vs. | 02/2022 | 0.011784275 |
| 07/2021 | vs. | 03/2022 | 0.010866307 |

| | | | |
|---|---|---|---|
| 07/2021 | vs. | 04/2022 | 0.010958215 |
| 08/2021 | vs. | 09/2021 | 0.009836136 |
| 08/2021 | vs. | 10/2021 | 0.009655373 |
| 08/2021 | vs. | 11/2021 | 0.009329317 |
| 08/2021 | vs. | 12/2021 | 0.008012712 |
| 08/2021 | vs. | 01/2022 | 0.008755749 |
| 08/2021 | vs. | 02/2022 | 0.008885443 |
| 08/2021 | vs. | 03/2022 | 0.008582609 |
| 08/2021 | vs. | 04/2022 | 0.008412405 |
| 09/2021 | vs. | 10/2021 | 0.000852665 |
| 09/2021 | vs. | 11/2021 | 0.001248771 |
| 09/2021 | vs. | 12/2021 | 0.002843747 |
| 09/2021 | vs. | 01/2022 | 0.003033719 |
| 09/2021 | vs. | 02/2022 | 0.00366234 |
| 09/2021 | vs. | 03/2022 | 0.002565095 |
| 09/2021 | vs. | 04/2022 | 0.002886546 |
| 10/2021 | vs. | 11/2021 | 0.001241123 |
| 10/2021 | vs. | 12/2021 | 0.002755377 |
| 10/2021 | vs. | 01/2022 | 0.003060635 |
| 10/2021 | vs. | 02/2022 | 0.003586108 |
| 10/2021 | vs. | 03/2022 | 0.002433799 |
| 10/2021 | vs. | 04/2022 | 0.00284005 |
| 11/2021 | vs. | 12/2021 | 0.002388943 |
| 11/2021 | vs. | 01/2022 | 0.00288705 |
| 11/2021 | vs. | 02/2022 | 0.003697546 |
| 11/2021 | vs. | 03/2022 | 0.002604065 |
| 11/2021 | vs. | 04/2022 | 0.0029291 |
| 12/2021 | vs. | 01/2022 | 0.002855218 |
| 12/2021 | vs. | 02/2022 | 0.003199097 |
| 12/2021 | vs. | 03/2022 | 0.002500856 |
| 12/2021 | vs. | 04/2022 | 0.002605507 |
| 01/2022 | vs. | 02/2022 | 0.001098437 |
| 01/2022 | vs. | 03/2022 | 0.001284685 |
| 01/2022 | vs. | 04/2022 | 0.001521723 |
| 02/2022 | vs. | 03/2022 | 0.001337254 |
| 02/2022 | vs. | 04/2022 | 0.001516877 |
| 03/2022 | vs. | 04/2022 | 0.000897109 |

Appendix E: Groups of Months $G_Y$ Matrices Comparisons

*Table E.1:* ADV*s for every* $\mathrm{G_Y}$ *with every other* $\mathrm{G_Y}$ *for four TOD periods (*t *= 1, 2, 3, 4)*

| | | | TOD period | | | |
|---|---|---|---|---|---|---|
| $G_Y$' | $G_Y$ | | 7-11AM | 11AM-3PM | 3-6PM | 6-9PM |
| 1 | 2 | | 0.006809436 | 0.010571241 | 0.009344097 | 0.014974756 |
| 1 | 3 | | 0.012647126 | 0.010099925 | 0.011703289 | 0.014772465 |
| 1 | 4 | * | 0.019417156 | 0.013130053 | 0.016169829 | 0.02131599 |
| 1 | 5 | | 0.012412442 | 0.009448915 | 0.013450338 | 0.019474516 |
| 1 | 6 | | 0.014790466 | 0.014050303 | 0.016509283 | 0.01894937 |
| 1 | 7 | * | 0.010382141 | 0.00972019 | 0.01090699 | 0.013933768 |
| 1 | 8 | | 0.010447832 | 0.010449854 | 0.010753636 | 0.012471278 |
| 1 | 9 | | 0.015193799 | 0.012206732 | 0.013521928 | 0.016547371 |
| 1 | 10 | * | 0.012216021 | 0.011482295 | 0.012606213 | 0.014486944 |
| 1 | 11 | | 0.010986558 | 0.012158841 | 0.010978392 | 0.013383279 |
| 1 | 12 | | 0.014945593 | 0.012393965 | 0.013482563 | 0.016795019 |
| 2 | 3 | | 0.011280376 | 0.008933718 | 0.009273829 | 0.010800558 |
| 2 | 4 | | 0.019782426 | 0.016341514 | 0.015289978 | 0.022492956 |
| 2 | 5 | * | 0.013588842 | 0.00802033 | 0.010004794 | 0.01122501 |
| 2 | 6 | | 0.013544964 | 0.012229914 | 0.013197648 | 0.013968397 |
| 2 | 7 | | 0.011749118 | 0.012464465 | 0.010999931 | 0.015987714 |
| 2 | 8 | * | 0.009051563 | 0.009357275 | 0.008850514 | 0.013823734 |
| 2 | 9 | | 0.014001845 | 0.010764134 | 0.01116723 | 0.012010754 |
| 2 | 10 | | 0.012350345 | 0.010999569 | 0.011557817 | 0.01470191 |
| 2 | 11 | * | 0.009552669 | 0.007526815 | 0.008533504 | 0.011097788 |
| 2 | 12 | | 0.013413639 | 0.010580498 | 0.010576176 | 0.013059817 |
| 3 | 4 | | 0.021409481 | 0.015325038 | 0.015474306 | 0.023404572 |
| 3 | 5 | | 0.01617881 | 0.008651498 | 0.010055965 | 0.01344964 |
| 3 | 6 | * | 0.009890181 | 0.010627057 | 0.011399382 | 0.011362246 |
| 3 | 7 | | 0.008740975 | 0.008173087 | 0.01005762 | 0.013744794 |
| 3 | 8 | | 0.009353328 | 0.008814286 | 0.008057329 | 0.010505144 |
| 3 | 9 | * | 0.006715861 | 0.005356929 | 0.006294108 | 0.007201427 |
| 3 | 10 | | 0.008871665 | 0.007676526 | 0.009067693 | 0.011438847 |
| 3 | 11 | | 0.009463385 | 0.008816176 | 0.008775943 | 0.009081557 |

| | | | | | | |
|---|---|---|---|---|---|---|
| 3 | 12 | * | 0.005285618 | 0.004800092 | 0.005042328 | 0.006363159 |
| 4 | 5 | | 0.009298959 | 0.012320503 | 0.009316571 | 0.015492499 |
| 4 | 6 | | 0.020834181 | 0.017470009 | 0.018084155 | 0.02194644 |
| 4 | 7 | * | 0.0182051 | 0.013703653 | 0.013204659 | 0.013849141 |
| 4 | 8 | | 0.018128288 | 0.013088817 | 0.012154497 | 0.014866967 |
| 4 | 9 | | 0.018875058 | 0.015326721 | 0.013866348 | 0.019579856 |
| 4 | 10 | * | 0.020468543 | 0.015586877 | 0.015408719 | 0.016744882 |
| 4 | 11 | | 0.019297505 | 0.014620701 | 0.014899002 | 0.019405352 |
| 4 | 12 | | 0.020242186 | 0.016194918 | 0.015070091 | 0.020354697 |
| 5 | 6 | | 0.017121536 | 0.012364322 | 0.014664763 | 0.016768084 |
| 5 | 7 | | 0.012529963 | 0.010248336 | 0.012383334 | 0.015309954 |
| 5 | 8 | * | 0.012573386 | 0.010075764 | 0.011165772 | 0.012794228 |
| 5 | 9 | | 0.016390189 | 0.010912354 | 0.011638752 | 0.013780293 |
| 5 | 10 | | 0.01514815 | 0.010415203 | 0.012197279 | 0.016018702 |
| 5 | 11 | * | 0.014000074 | 0.010183902 | 0.010368186 | 0.014544119 |
| 5 | 12 | | 0.016531728 | 0.011031168 | 0.011492267 | 0.014370212 |
| 6 | 7 | | 0.008335513 | 0.009154008 | 0.01165719 | 0.013861199 |
| 6 | 8 | | 0.00918806 | 0.011623302 | 0.010870097 | 0.01131378 |
| 6 | 9 | * | 0.010526341 | 0.011056498 | 0.011138173 | 0.01097896 |
| 6 | 10 | | 0.008296735 | 0.009904387 | 0.011707785 | 0.013599977 |
| 6 | 11 | | 0.00892428 | 0.012091988 | 0.012000652 | 0.010207582 |
| 6 | 12 | * | 0.009547657 | 0.010887446 | 0.009768904 | 0.010330042 |
| 7 | 8 | | 0.004707329 | 0.007489218 | 0.005387711 | 0.010019962 |
| 7 | 9 | | 0.0109368 | 0.009701763 | 0.011403791 | 0.013401381 |
| 7 | 10 | * | 0.004593864 | 0.005712805 | 0.005357872 | 0.007233053 |
| 7 | 11 | | 0.005848087 | 0.009390277 | 0.00823076 | 0.010041032 |
| 7 | 12 | | 0.00988078 | 0.009756157 | 0.011196953 | 0.012696842 |
| 8 | 9 | | 0.010939418 | 0.00958914 | 0.009720286 | 0.011419096 |
| 8 | 10 | | 0.006995634 | 0.008912108 | 0.006913831 | 0.01126996 |
| 8 | 11 | * | 0.003649227 | 0.00605951 | 0.00623703 | 0.009396168 |
| 8 | 12 | | 0.009814694 | 0.0099194 | 0.009528834 | 0.01054111 |
| 9 | 10 | | 0.009500607 | 0.008505153 | 0.009579045 | 0.010561511 |
| 9 | 11 | | 0.008457606 | 0.008723605 | 0.007704307 | 0.008375212 |
| 9 | 12 | * | 0.003688221 | 0.003040129 | 0.003997356 | 0.005875444 |
| 10 | 11 | | 0.005989876 | 0.006284409 | 0.00522267 | 0.007825714 |
| 10 | 12 | | 0.0094051 | 0.009055527 | 0.009702509 | 0.010564186 |
| 11 | 12 | | 0.009550179 | 0.009788856 | 0.008773003 | 0.009728193 |

* between same $G_M$

Appendix F: *ADV*s for Comparisons Within the Same $G_M$ Organized by $G_M$

*Table F.1:* ADV*s for comparisons within* $G_M$ *= 1 organized from lowest to highest*

| $G_Y$' | $G_Y$ | ADV | *t* |
|---|---|---|---|
| 7 | 10 | 0.004593864 | 1 |
| 7 | 10 | 0.005357872 | 3 |
| 7 | 10 | 0.005712805 | 2 |
| 7 | 10 | 0.007233053 | 4 |
| 1 | 7 | 0.00972019 | 2 |
| 1 | 7 | 0.010382141 | 1 |
| 1 | 7 | 0.01090699 | 3 |
| 1 | 10 | 0.011482295 | 2 |
| 1 | 10 | 0.012216021 | 1 |
| 1 | 10 | 0.012606213 | 3 |
| 1 | 4 | 0.013130053 | 2 |
| 4 | 7 | 0.013204659 | 3 |
| 4 | 7 | 0.013703653 | 2 |
| 4 | 7 | 0.013849141 | 4 |
| 1 | 7 | 0.013933768 | 4 |
| 1 | 10 | 0.014486944 | 4 |
| 4 | 10 | 0.015408719 | 3 |
| 4 | 10 | 0.015586877 | 2 |
| 1 | 4 | 0.016169829 | 3 |
| 4 | 10 | 0.016744882 | 4 |
| 4 | 7 | 0.0182051 | 1 |
| 1 | 4 | 0.019417156 | 1 |
| 4 | 10 | 0.020468543 | 1 |
| 1 | 4 | 0.02131599 | 4 |

*Table F.2:* ADV*s for comparisons within* $G_M$ *= 2 organized from lowest to highest*

| $G_Y$' | $G_Y$ | ADV | *t* |
|---|---|---|---|
| 8 | 11 | 0.003649227 | 1 |
| 8 | 11 | 0.00605951 | 2 |
| 8 | 11 | 0.00623703 | 3 |
| 2 | 11 | 0.007526815 | 2 |
| 2 | 5 | 0.00802033 | 2 |
| 2 | 11 | 0.008533504 | 3 |
| 2 | 8 | 0.008850514 | 3 |
| 2 | 8 | 0.009051563 | 1 |
| 2 | 8 | 0.009357275 | 2 |
| 8 | 11 | 0.009396168 | 4 |
| 2 | 11 | 0.009552669 | 1 |
| 2 | 5 | 0.010004794 | 3 |
| 5 | 8 | 0.010075764 | 2 |
| 5 | 11 | 0.010183902 | 2 |
| 5 | 11 | 0.010368186 | 3 |
| 2 | 11 | 0.011097788 | 4 |
| 5 | 8 | 0.011165772 | 3 |
| 2 | 5 | 0.01122501 | 4 |
| 5 | 8 | 0.012573386 | 1 |
| 5 | 8 | 0.012794228 | 4 |
| 2 | 5 | 0.013588842 | 1 |
| 2 | 8 | 0.013823734 | 4 |
| 5 | 11 | 0.014000074 | 1 |
| 5 | 11 | 0.014544119 | 4 |

*Table F.3:* ADV*s for comparisons within* $G_M$ *= 3 organized from lowest to highest*

| $G_Y$' | $G_Y$ | ADV | $t$ |
|---|---|---|---|
| 9 | 12 | 0.003040129 | 2 |
| 9 | 12 | 0.003688221 | 1 |
| 9 | 12 | 0.003997356 | 3 |
| 3 | 12 | 0.004800092 | 2 |
| 3 | 12 | 0.005042328 | 3 |
| 3 | 12 | 0.005285618 | 1 |
| 3 | 9 | 0.005356929 | 2 |
| 9 | 12 | 0.005875444 | 4 |
| 3 | 9 | 0.006294108 | 3 |
| 3 | 12 | 0.006363159 | 4 |
| 3 | 9 | 0.006715861 | 1 |
| 3 | 9 | 0.007201427 | 4 |
| 6 | 12 | 0.009547657 | 1 |
| 6 | 12 | 0.009768904 | 3 |
| 3 | 6 | 0.009890181 | 1 |
| 6 | 12 | 0.010330042 | 4 |
| 6 | 9 | 0.010526341 | 1 |
| 3 | 6 | 0.010627057 | 2 |
| 6 | 12 | 0.010887446 | 2 |
| 6 | 9 | 0.01097896 | 4 |
| 6 | 9 | 0.011056498 | 2 |
| 6 | 9 | 0.011138173 | 3 |
| 3 | 6 | 0.011362246 | 4 |
| 3 | 6 | 0.011399382 | 3 |

Appendix G: Plots of *ADV*s for $G_Y$ Comparisons Within the Same $G_M$ Organized by Pandemic Timeframe

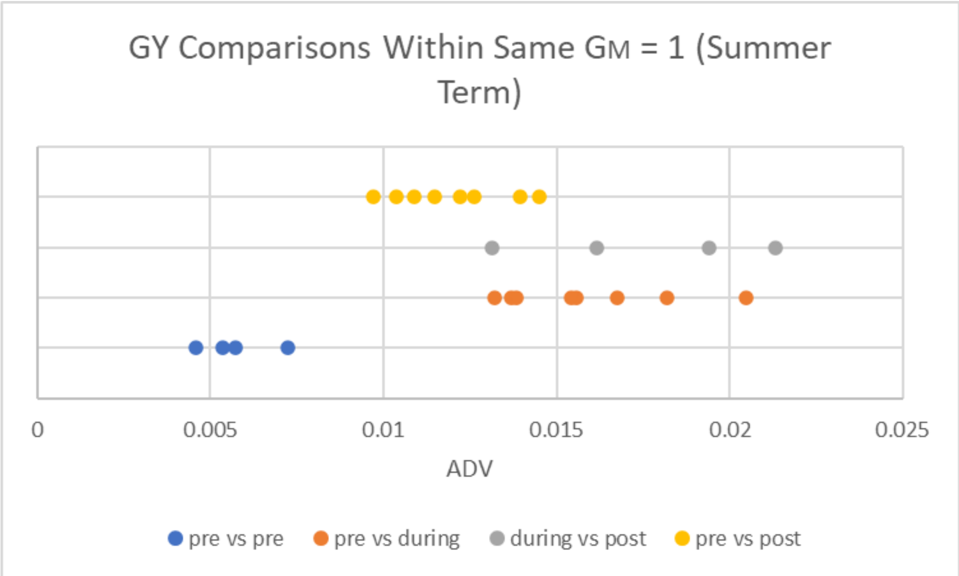


*Figure G.1: Plot of* ADVs *for comparisons between* $G_Y$s *belonging to the same* $G_M$ *= 1 (summer term)*

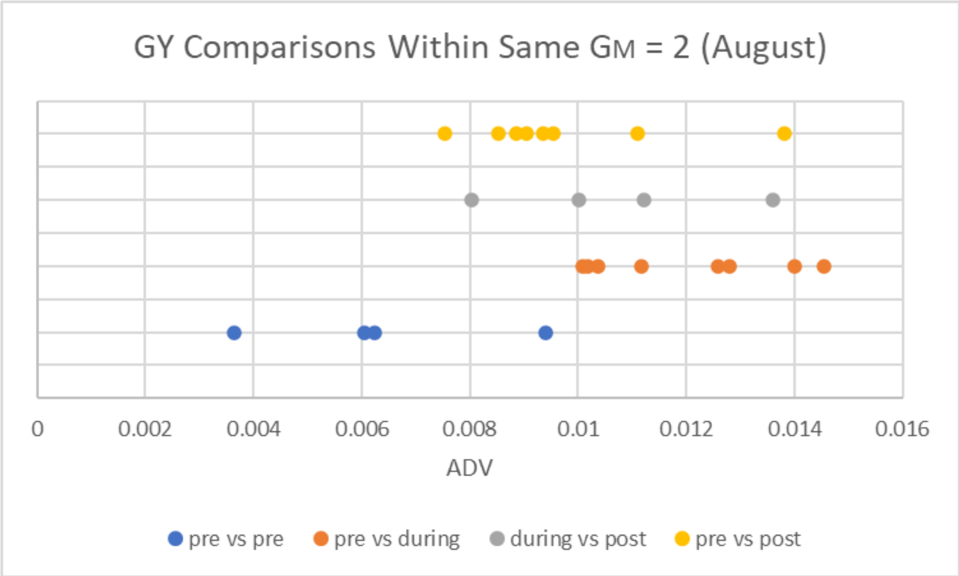


*Figure G.2: Plot of* ADVs *for comparisons between* $G_Y$s *belonging to the same* $G_M$ *= 2 (August)*

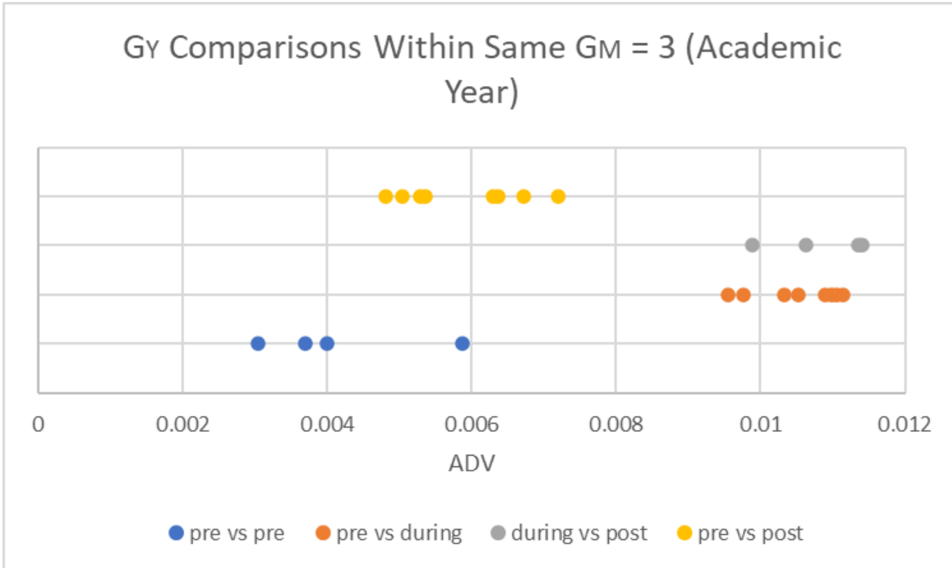


*Figure G.3: Plot of* ADVs *for comparisons between* $G_Y$*s belonging to the same* $G_M$ *= 3 (academic year)*